Fiber Reinforced Concrete Connections for Earthquake Resistant Design of Precast Reinforced Concrete Structures

by
Khaled S. Soubra
James K. Wight
Antoine E. Naaman

A Report on Research Sponsored by
National Science Foundation
Grant No. CES-86-15419

Report No. UMCE 89-13
October 1989

Department of Civil Engineering
The University of Michigan
Ann Arbor, MI 48109-2125

Fiber Reinforced Concrete Connections for Earthquake Resistant Design of Precast Reinforced Concrete Structures

by
Khaled S. Soubra
James K. Wight
Antoine E. Naaman

A Report on Research Sponsored by
National Science Foundation
Grant No. CES-86-15419

Report No. UMCE 89-13
October 1989

Department of Civil Engineering
The University of Michigan
Ann Arbor, MI 48109-2125

ABSTRACT

This investigation is part of a comprehensive study aimed at developing a strong, ductile, and energy dissipating connection for precast concrete members in seismic zones. The strength, ductility, and energy dissipation of the connection were provided through a cast-in-place (CIP) fiber reinforced concrete (FRC) composite placed between the precast concrete elements.

In the first part of the investigation, cylindrical specimens of FRC composites were tested under compression in order to select an adequate composite for the CIP joint.

In the second part of the investigation, six beam-type specimens, in which the fiber reinforced CIP joint was placed between the precast elements, were tested under cyclic third point loading. A localized failure was observed for all the specimens in the CIP joint. This failure was due to the opening of a single major crack in each specimen, causing stress concentration in the reinforcing bars, which led to snapping of at least one of these bars and, hence, failure of that specimen. However, despite the localized failure, the plastic hinging zone exhibited good ductility and energy dissipation.

ACKNOWLEDGMENTS

This investigation was supported by the National Science Foundation Grant No. CES-86-15419 to the University of Michigan with Dr. S. C. Liu as NSF program director. The authors are very grateful for that support. Any opinions, findings, and conclusions expressed in this paper are those of the authors and do not necessarily reflect the views of the sponsor.

TABLE OF CONTENTS

LIST OF FIGURES

Figure

LIST OF TABLES

Table

CHAPTER I

INTRODUCTION

1.1 -General

Precast concrete elements are widely used as structural elements in non-seismic areas because of their construction efficiency and saving in time and costs. However, these elements are not widely used in seismic areas (6,10,12,13,14). This can be related to prior poor performance of precast structures during earthquakes, and also due to the lack of design recommendations for connections between precast concrete members in highly seismic areas. The objective of the proposed research is to examine the possibility of obtaining a ductile and energy dissipating connection between precast elements, and to develop design techniques for precast concrete connections.

The design of precast and cast-in-place concrete structures in seismic zones has two main objectives : a) preventing loss of life and b) limiting structural damage. In order to satisfy these requirements, design recommendations have been proposed for cast-in-place reinforced concrete structures (3,7,21). These recommendations are the result of studies on the behavior of reinforced concrete structures under earthquake loads. A

reinforced concrete structure in a seismic zone is expected to experience damage during a severe earthquake. The structure is subjected to forces beyond its elastic limit and as a result, inelastic deformations occur in the critical regions.

Beam to column connections are considered to be critical regions in a reinforced concrete frame. The testing of these connections provides relevant information about the behavior of the structure under earthquake loads, Fig. 1.1. Test results show that under cyclic loading, plastic hinges form adjacent to the column faces. These hinges form in order to dissipate the input energy, and through their inelastic rotation, they provide ductility to the structure.

However, the location of beam plastic hinges adjacent to columns can cause stiffness degradation, loss of strength, and reduction in the column capacity. A related consequence is the high bond stress in the beam reinforcing bars passing through the column due to the penetration of yield strains. As a result, these bars can either pull out from an exterior joint or slip through an interior joint.

In order to retain the strength and stiffness of the joint, the current design recommendations (21) require a high percentage of transverse reinforcement in the column as it passes through the joint. This leads to congestion of steel in the connection and consequently increases in construction time and cost. Such problems are avoided if the joint can maintain an elastic behavior throughout the loading history.

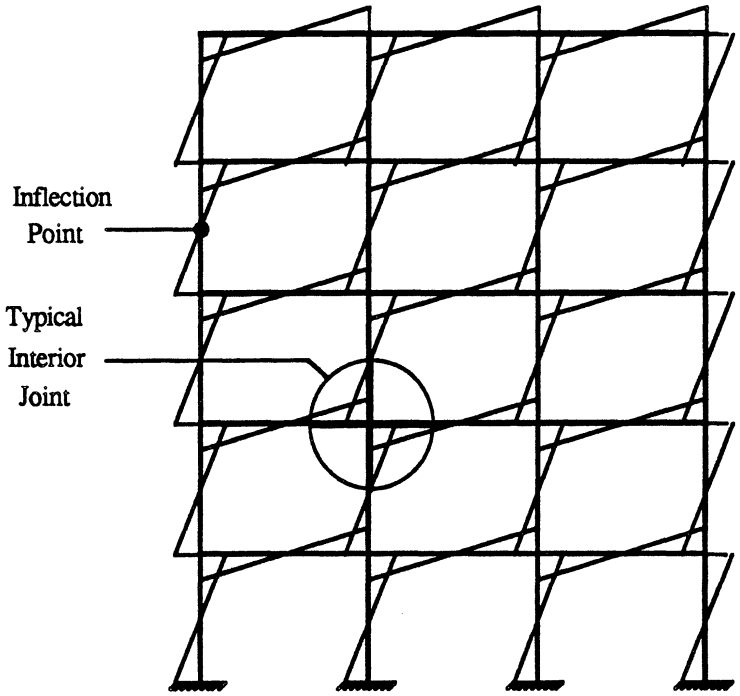

a) Moments due to Earthquake Loading

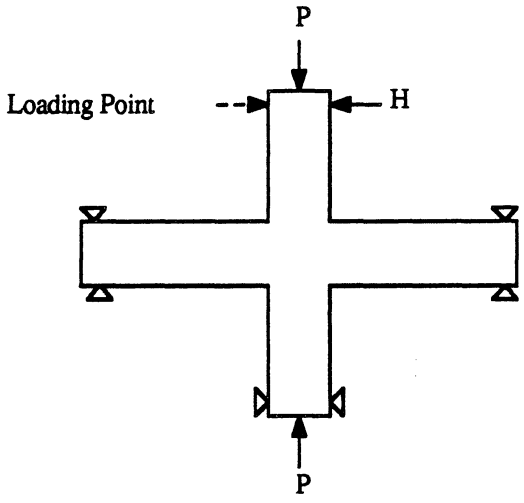

b) Interior beam-to-column connection

Fig. 1.1- Typical testing setup for beam-to-column connections.

Elastic behavior of the joint can be achieved by moving the beam plastic hinge away from the face of the column. This would help reduce the amount of transverse reinforcement required by the Code (3), provided that shear strength requirements are met. Furthermore, it would help retain the strength and stiffness of the joint as well as the column capacity. Relocating the plastic hinge away from the column face would also keep inelastic strains from penetrating into the joint core which would reduce the bond stresses in the beam reinforcing bars. This alternative solution can be applied to precast concrete elements as well as cast-in-place reinforced concrete.

In the case of cast-in-place reinforced concrete connections, the relocation of the plastic hinge can be achieved by providing a special reinforcement layout at the proposed plastic hinge location (1). A similar reinforcement detail can be used for a cast-in-place connection region between precast beam and column elements. However, because this connection region is expected to experience large inelastic deformations and dissipate energy, a tougher and more ductile concrete material can be used. For this research project, a fiber reinforced concrete was used.

CHAPTER II

Review of Previous Research

Many researchers have studied the behavior of beam-to-column connections. Extensive experimental work was conducted to observe the behavior of the connection, identify the problems, and propose potential solutions. In the report "Recommendations for Design of Beam-to-Column Joints in Monolithic Reinforced Concrete Structures", the ACI-ASCE joint committee 352 (22) identified four major design problems: 1) confinement of the joint core; 2) shear strength of the joint core; 3) beam-to-column flexural strength ratio; and 4) anchorage of beam bars terminating in the joint. In order to solve those problems, design recommendations were proposed, among which was to increase the amount of transverse reinforcement in the joint and limit the nominal shear capacity of the joint.

Paulay and Park (21) also reported the need to provide adequate shear reinforcement in the joint core and to set an upper limit to the value of shear stresses developed in the core. It was found that providing adequate shear reinforcement would help: 1) transfer the forces from

adjacent members under large load reversals without significant reduction in stiffness and energy dissipation; 2) prevent shear failure by diagonal tension; and 3) prevent slippage of beam bars through the joint due to bond failure. The upper limit to the value of shear stresses developed in the joint was set to prevent crushing of the concrete in the diagonal compression strut under large load reversals when a large amount of transverse reinforcement is provided.

Durrani and Wight (11) studied the effect of the transverse reinforcement and the level of joint shear stress on the behavior of the joint. They reported that a higher percentage of transverse reinforcement produced better confinement for the joint core. Consequently, the connection suffered less shear deformation and exhibited better energy dissipation for all the ductility levels considered. Durrani and Wight also reported that a lower level of joint shear stresses: 1) provided significantly improved energy dissipation and "superior hysteretic behavior"; 2) maintained stiffness and load carrying capacity; and 3) prevented joint shear failure.

Lee, Wight, and Hanson (19) studied the behavior of exterior beam-to-column connections under moderate and severe earthquake loadings. The specimens designed according to the recommendations of the Joint Committe ACI-ASCE 352 had a better overall behavior. The addition of transverse reinforcement in the beams according to the recommendations: 1) provided better confinement for the beam core; 2) reduced shear slippage and buckling of longitudinal reinforcement; and 3) provided better energy dissipation and less strength degradation. In the other

specimens, however, where inadequate transverse reinforcement was provided, large cracks opened and the plastic hinges were localized. The presence of large cracks caused shear slippage and consequently, a significant reduction in strength and energy dissipation.

Scribner and Wight (23) studied the effect of the introduction of intermediate longitudinal reinforcement in the beams on the behavior of the joint under cyclic loading. The effects of shear span to depth ratio as well as the level of shear stress were also studied. It was reported that for members with low shear stress levels, flexural cracks developed with no significant shear slippage. Similar behavior was observed for long shear spans as opposed to short shear spans where a small plastic hinging zone and shear-related failure were noted. It was also reported that the use of intermediate longitudinal reinforcement in the beams provided: 1) a more effective confinement for the beam core; 2) a more uniform cracking distributed through the plastic hinge region; 3) a prolonged and stable hysteretic behavior; and 4) a significantly increased energy dissipation.

In an experimental study, Abdel-Fattah and Wight (1) studied the possibility of improving the behavior of the joint by moving the plastic hinge away from the face of the column. This was done by introducing intermediate longitudinal reinforcement in the beam, extending 1.5 times the beam depth from the column face on each side of the joint Fig. 2.1. It was observed that relocating the beam plastic hinging zone provided higher energy dissipation, little or no strength decay, and reduced pinching of moment vs. rotation hyteresis loops.

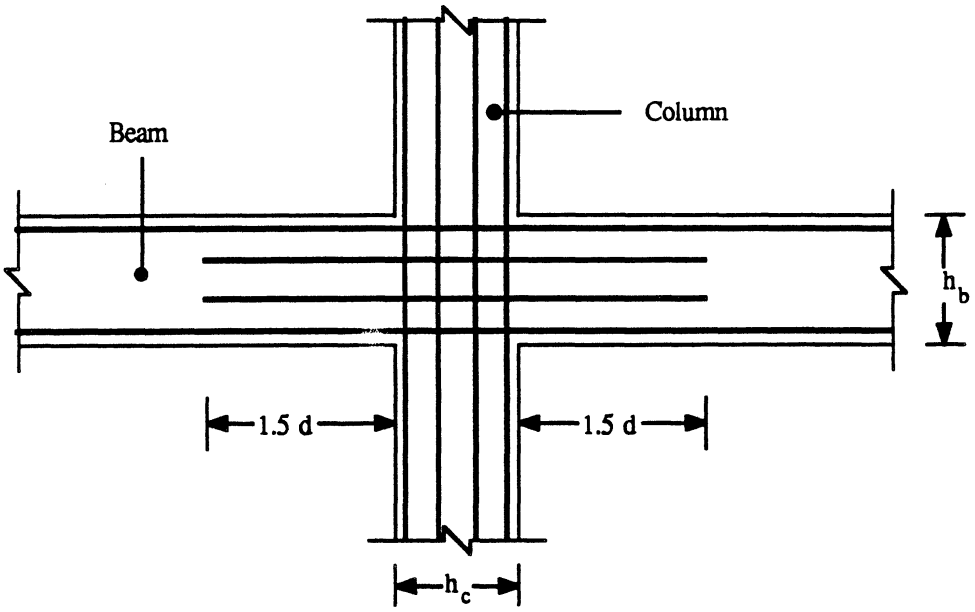

Fig. 2.1- Steel arrangement. (1)

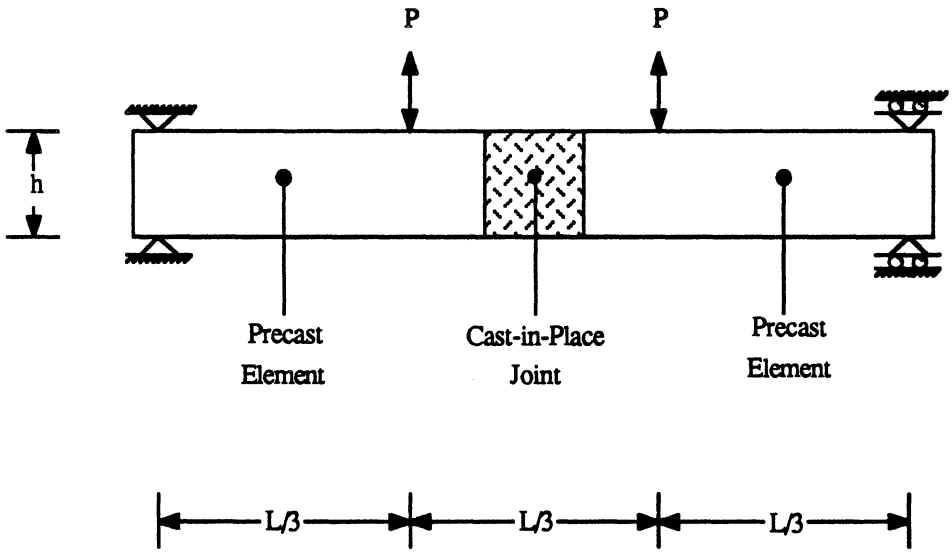

Fig. 2.2- Beam-type specimens. (2)

The improved behavior was related to the fact that the beam section adjacent to the column faces behaved elastically under repeated cyclic loading since: 1) beam concrete compression forces were sustained and contributed to the transfer of forces; 2) beam reinforcement yielding did not penetrate in the joint core; and 3) adequate bond stresses were developed in the joint core. It was also noted that the use of intermediate longitudinal reinforcement in the beam eliminated sliding shear deformations and that the relocation of the plastic hinge away from the column face reduced the amount of transverse reinforcement required in the joint core.

Abdou, Naaman, and Wight (2) studied the possibility of relocating the plastic hinge in precast prestressed concrete elements. Twelve specimens were tested in this study. The specimens were beam-type specimens as shown in Fig. 2.2. Each beam consisted of two precast, concrete elements joined together at the connector using SIFCON (Slurry Infiltrated Fiber Concrete). SIFCON was used as the matrix at the proposed hinge location since a strong, ductile, and good energy dissipating connector between the precast elements was required (6). Different reinforcing steel configurations were used in the joint, as shown in Fig. 2.3, to ensure the occurence of the plastic hinge in the connector under cyclic loading. The connector was subjected to constant moment and zero shear since third point loads were applied to the specimens. A good behavior under cyclic loading was reported for some specimens. The failure occurred in the cast-in-place SIFCON joint and an elastic behavior was maintained outside the cast-in-place joint.

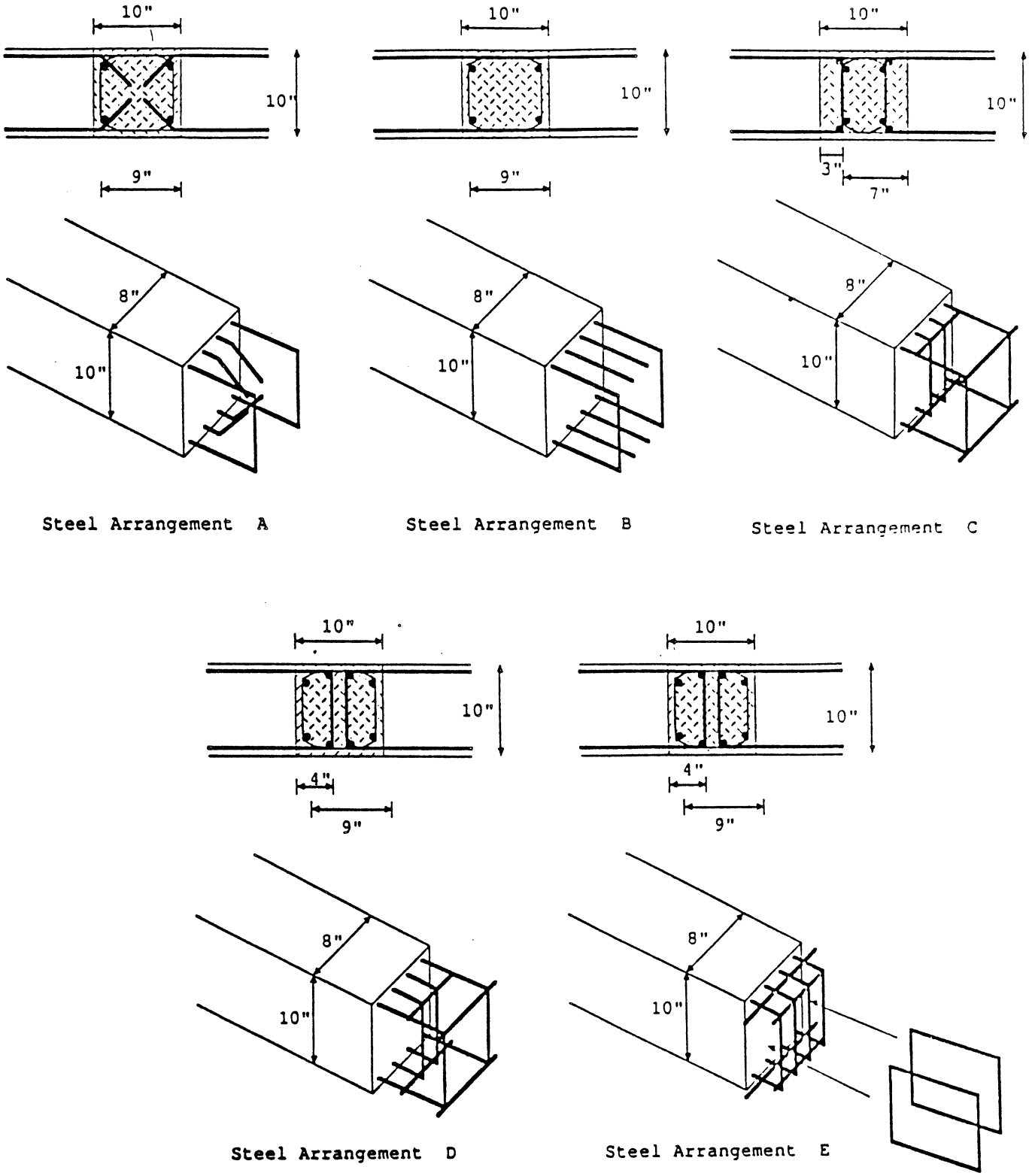

Fig. 2.3- Reinforcing steel configurations.

Furthermore, good ductility and energy dissipation were observed despite localized failure which contributed to stiffness degradation and pinching in the load vs. displacement hysteresis loops.

The demand for high ductility, strength, and energy dissipation in beam-to-column connections under cyclic loading has led many investigators into studying the substitution of conventional concrete in the connection area with steel fiber reinforced concrete (8,15,17,18,24). Fiber reinforced concrete is a composite consisting of discontinuous discrete steel fibers in addition to the cement paste, sand and aggregate. This composite has significantly improved mechanical properties such as static strength, which includes ductility and toughness, as well as dynamic and fatigue strength (4). The use of fiber reinforced concrete in individual structural elements such as beams and columns has improved the behavior of these elements (9,16).

Jindal (16) reported that substituting for conventional reinforced concrete in beams with steel fiber reinforced concrete increased the shear and flexural strength as well as the toughness of the beams. In his study involving the testing of 44 beams, different fibers aspect ratios (l/d) were used, while the volume content of fibers V_f was kept constant at 1%. The best results were observed when fibers of aspect ratio of 75 were used. A method for analysis and design of steel fiber reinforced concrete beams was also suggested.

The use of fiber reinforced concrete in beam-to-column connections was investigated as well as individual structural elements. Jindal and

Sharma (18) tested 92 knee-type SFRC beam-to-column connections to determine the effect of steel fibers on their behavior. Different fibers aspect ratios (l/d = 10 to 100), volume content of fibers (V_f = 0.5 to 2.0 %), as well as different types of fibers were used. Increases were reported in ductility, toughness, strength, moment capacity, energy dissipation, as well as crack resistance and ultimate rotation. The influence of the type, aspect ratio, and volume content of fibers on the behavior of the connections was also observed.

Sood and Gupta (24) tested 50 beam-to-column connections of conventional and fiber reinforced concrete under static, as well as slow cycle fatigue loading. A single value of fibers aspect ratio was used (l/d = 100) for different volume contents of fibers (V_f = 0.0, 0.6, 0.8, 1.0 %). A significant improvement was reported in the performance of SFRC (Steel Fiber Reinforced Concrete) connections over conventional connections. The SFRC connections exhibited increased ductility, stiffness, load carrying capacity, ultimate rotational capacity, as well as better damage tolerance.

Craig et al. (8) tested 10 beam-to-column connections where SFRC was used in the joint area. Hooked end steel fibers with different aspect ratios (l/d = 60, 100), and a volume fraction V_f of 1.5 % were used. Observations similar to the previous ones were made about the behavior of the connection. It was concluded that the fibers in the joint provided more ductility and stiffness, higher shear and moment strength, and better energy dissipation as well as better bond and concrete confinement. It was recommended that fiber reinforced concrete be used in the critical

regions in seismic resistant buildings since its use in such regions proved to yield a safer and more economical design. Other investigators tested SFRC beam-to-column connections with different types, aspect ratios, and volume content of fibers (15,17). These tests drew conclusions which were very similar to conclusions in the previous studies, all of which proved the advantages and benefits, as well as recommended the use of SFRC in the connection.

As "performance related" features, such as energy dissipation, strength, and ductility, are desired in reinforced concrete structures in seismic areas, so are other "construction related" features, such as good quality control, ease and speed of construction, and saving in constuction costs. The use of precast concrete elements in construction provides such benefits. However, the wide spread use of precast concrete is limited to non-seismic areas and is still somewhat unacceptable in seismic areas due to many factors such as: 1) the abscence of special provisions in the North American design codes for the seismic design of precast concrete structures, therefore forcing the use of the provisions developed for cast-in-place concrete structures; and 2) the abscence of a practical method for connecting the elements and satisfying requirements of adequate strength, ductility, and energy dissipation under cyclic loading.

Many concepts for the development of earthquake resistant ductile connections using precast concrete have been investigated (13,14). Dolan et al. (10) tested beam-to-column connections made out of precast concrete elements. Several methods were used in assembling the precast elements such as field welding, continuous reinforcing, bolting, post tensioning,

grouting, etc. In one specimen, the precast beam member was connected to a cast-in-place column. It was reported that although the strength of all the connections at least equaled the required strength, only the specimen connected to the cast-in-place column showed adequate energy dissipation while the rest showed low energy dissipation. The authors concluded that more detailing and "imaginative design" is needed to improve the behavior of the connections. Additional experimental work is also needed since the data available was the result of testing only one specimen of each assembly method from which no definite conclusions can safely be drawn.

It is the purpose of this research to combine the use of precast concrete with fiber reinforced cast-in-place concrete in beam-to-column connections to provide a better, safer, and more economical design. This research will also investigate moving the plastic hinge, in other words, moving the connection between the precast elements away from the face of the column. At that location, the design requirements such as ductility, strength, and energy dissipation would be provided by the cast-in-place fiber reinforced concrete connection.

CHAPTER III

EXPERIMENTAL PROGRAM

PART I : CYLINDERS TESTS

3.1 -General

The experimental program consisted of two parts. The first part was aimed at designing and selecting a suitable FRC composite that could provide the required properties for a cast-in-place joint. This was achieved through the testing of different fiber reinforced concrete composites. The second part consisted of the testing of six beam-type specimens where the composite was used as a cast-in-place connection joining the precast concrete parts. A beam-type specimen is shown in Fig.3.1.

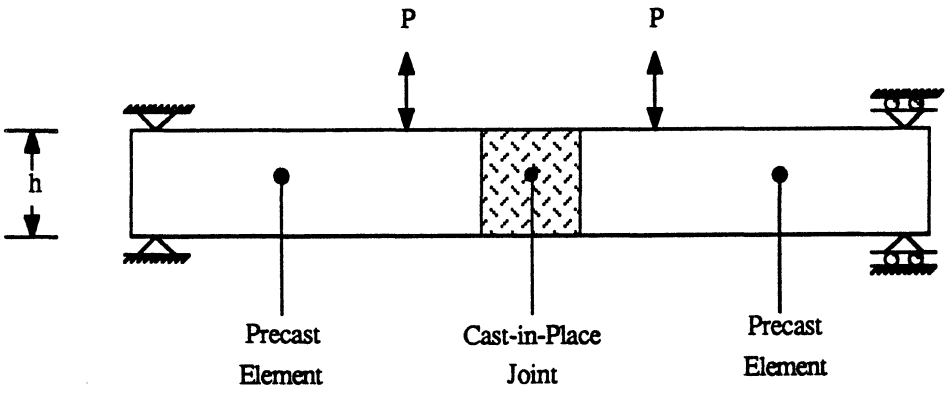

Fig. 3.1- Beam-type specimen.

3.2 -Design of FRC Composites

As mentioned earlier, FRC composites consist of cement paste, sand and/or aggregate, and discontinuous discrete fibers. Variations in the composite components lead to changes in its mechanical properties, such as strength and toughness. FRC cylinders were cast and tested under monotonic compression loading to study the effect of parameter variation on the composite response, and, therefore, select an adequate FRC composite for the cast-in-place joints in the beam-type specimens. The parameters used in each composite are summarized in Table 3.1.a. Steel fibers were mostly used, except for two sets with polypropelene fibers, as noted in Table 3.1.a. The control specimens parameters are given in Table 3.1.b. The cylinders were grouped in three series: Series I, Series II, and Series III.

3.2.1 -Preparation of Cylinders

All cylinders were prepared following ASTM (American Society for Testing Materials) specifications. ASTM Type I cement and 2NS sand were used in Series I & II. Coarse aggregate was used in addition to sand in Series III. This coarse aggregate was crushed limestone with a nominal maximum size of 3/8 in.

Three cylinders were cast and tested for each composite; the resulting stress-strain curves were then averaged to provide an average curve representing the compressive behavior of that composite. The composite components were mixed in an industrial food mixer having a maximum capacity of 2/3 cubic foot. For Series I & II, the mixing

Table 3.1- a) Composites Parameters.

Series	Name	Cylinder Dimensions *in. x in.*	Number of Cylinders	Matrix Components				Fibers		
				Cement	Sand	Aggregate	Water	Name	Length	Vol. Fraction
I	POLYC1S4	4 x 8	3	1	1	---	0.5	Polypropelene	3/4 in.	4.00%
	FLATC1S4	4 x 8	3	1	1	---	0.5	Flat	3/4 in.	4.00%
	CRMPC1S4	4 x 8	3	1	1	---	0.5	Crimped	1.0 in.	4.00%
	HOKDC1S4	4 x 8	3	1	1	---	0.5	Hooked	30 mm	4.00%
	DFMDC1S4	4 x 8	3	1	1	---	0.5	Deformed	30 mm	4.00%
II	HOKDC2S4	4 x 8	3	1	2	---	0.5	Hooked	30 mm	4.00%
	DFMDC2S4	4 x 8	3	1	2	---	0.5	Deformed	30 mm	4.00%
III	HOKDC2S4	4 x 8	3	1	2	---	0.5	Hooked	30 mm	4.00%
	DFMDC2S4	4 x 8	3	1	2	---	0.5	Deformed	30 mm	4.00%
	POLYC1S4	4 x 8	3	1	1	---	0.5	Polypropelene	3/4 in.	4.00%
	HK50CONC	4 x 8	3	1	2.5	2.1	0.5	Hooked	50 mm	1.00%
	HK30CONC	4 x 8	3	1	2.5	2.1	0.5	Hooked	30 mm	2.10%
	DF30CONC	4 x 8	3	1	2.5	2.1	0.5	Deformed	30 mm	2.10%

Table 3.1- b) Control specimens parameters.

Name	Cylinder Dimensions *in. x in.*	Number of Cylinders	Matrix Components			
			Cement	Sand	Aggregate	Water
CONTROL I	4 x 8	3	1	1	---	0.5
CONTROL II	4 x 8	3	1	2	---	0.5
CONTROL III	4 x 8	3	1	2.5	2.1	0.5

sequence began by dry mixing the cement and sand and then adding water gradually. The fibers were then added in the same manner. A small amount of superplasticizer, trade named Melment, was added occasionally to maintain workability. For Series III, the cement and sand were dry mixed, then part of the water was added slowly. The coarse aggregate and fibers were then added alternatively in small amounts with additional water to maintain workability. Melment was also used to maintain workability after the complete specified amount of water had been added.

Once the mixing was done, the mix was cast into oiled cylinders and placed on a vibrator to ensure compaction. The cylinders were left to set for one day, after which they were removed from the molds and placed in water to cure for seven days. After seven days, the cylinders were removed from water to dry and then capped using Cyclap, a high strength sulfur compound, to ensure smooth loading surfaces. The cylinders were then stored in the laboratory until testing.

3.2.2 -Testing Aparatus and Data Acquisition System

The testing system is shown in Fig.3.2. A computer-controlled Universal Testing Machine (Instron System 8000) was used in the testing. The testing machine had a maximum hydraulic actuator capacity of 550 kips. The system was equipped with a Hewlett-Packard x-y recorder as well as a digital display mode to monitor the tests.

The tests were run under actuator displacement control at a strain rate of 125 microstrain per second (0.001 inch per second). The test data was read and stored by a data acquisition system. The load level was read

Fig. 3.2- Testing apparatus.

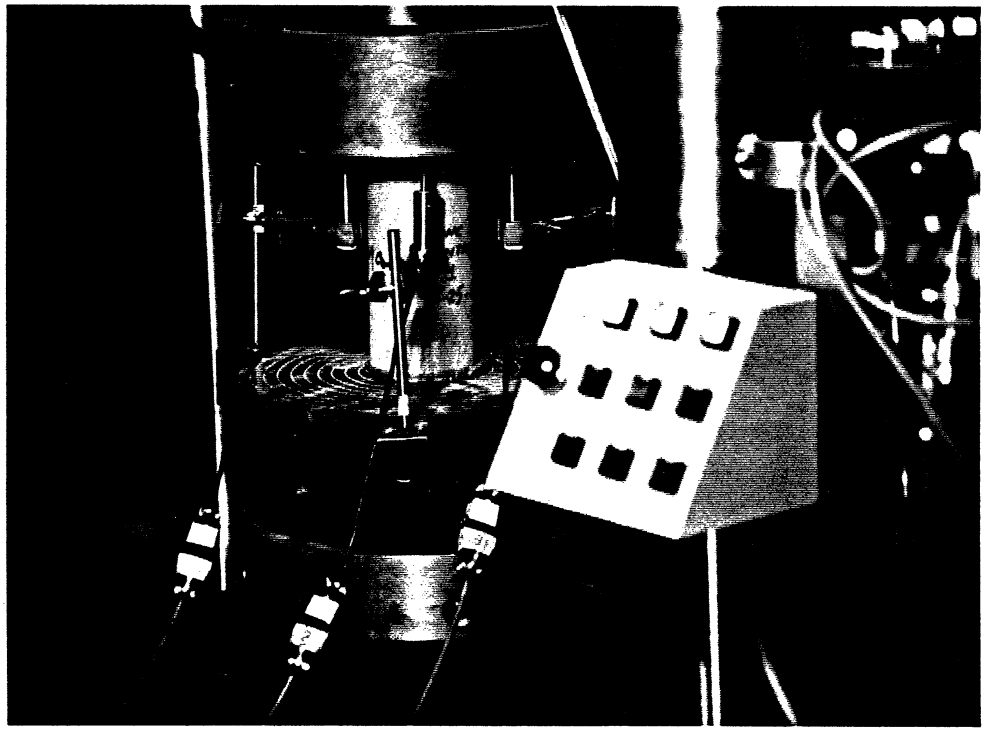

Fig. 3.3- LVDT configuration.

from a load cell, and the displacement was read from an LVDT inside the actuator. In Series III, more accurate readings of the cylinders deformations were obtained using three LVDT (Linear Variable Differential Transformers) placed around the cylinders at 120 degree spacing between the plattens of the testing machine. Fig.3.3 shows the LVDT arangement between the machine plattens.

3.3 -Series I Characteristics

3.3.1 -Mix Design

In the first series of cylinders, five types of fibers were added to a mortar mix: polypropelene plastic fibers, flat, crimped, hooked, and deformed steel fibers. The geometric properties of the fibers are summarized in Table 3.2. The purpose was to examine the possibility of obtaining a workable FRC composite containing a fiber volume fraction of 4%, since it is known that an increase in the fibers volume fraction would enhance the mechanical properties of the composite and provide the necessary strength, ductility, and energy dissipation in the CIP joint. Therefore, using the previously mentioned fibers, a fiber volume fraction of 4% was successfully placed in each mix. It was not possible, however, to place a higher percentage of fibers without the matrix becoming unworkable.

Three cylinders containing the mortar matrix and no fibers, refered to as control cylinders, were also cast. The control cylinders served as references.

Table 3.2- Fibers geometric properties.

Fiber Type	Supplier	Length	Cross-Section	Dimensions	Equiv. Diam.	l/d
Polypropelene	Fibermesh	19 mm	Circular	---	0.095 mm	200
Crimped	RIBTEC	25.4 mm	Circular / Xorex II	---	0.89 mm	30
Flat	Mitchell Fibercon	19 mm	Rectangular	0.25 x 0.56 mm	0.42 mm	45
Deformed	Surecrete	30 mm	Circular	---	0.5 mm	60
Hooked	Beakert Dramix	30 mm	Circular	---	0.5 mm	60
Hooked	Beakert Dramix	50 mm	Circular	---	0.5 mm	100

3.3.2 -Test Results

In discussing the test results for the FRC cylinders, the following quantities are of importance: the slope of the ascending branch of the stress-strain compression curve, also referred to as the stiffness or the modulus of elasticity; the value of the peak stress; and the area under the stress-strain curve (toughness). The area under the curve was calculated using the trapezoidal rule. A toughness index was obtained by normalizing the area under the curve of the fiber reinforced specimens with respect to the area under the curve of the control specimens.

Upon testing the cylinders, various results were obtained. The control specimens failed suddenly in a brittle manner, as expected, exhibiting a cone shaped failure surface. The average maximum compressive stress was 4200 psi. The test results of Series I are summarized in Table 3.3.

Crimped Steel Fibers in Mortar Matrix: (l=1in, V_f=4 %)

The stress-strain curve for the specimens containing crimped steel fibers is shown in Fig.3.4. The addition of these fibers did not improve either the the compressive stiffness or the compressive strength of the mortar mix. An average maximum compressive stress of only 4540 psi was obtained, the smallest observed among all the specimens of the first series. The crimped fiber specimens, however, exhibited some improvement in toughness with the compressive strength gradually

Table 3.3- Series I test results.

Name	Fibers * in Cylinder	Maximum Comp. Stress *(psi)*	Asymptotic Stress *(psi)*	Toughness Index
CONTROL I	---	4200	0	1.00
POLY4	Polypropelene	5670	560	3.14
CRM4	Crimped	4540	900	3.75
FLT4	Flat	6400	1100	5.41
DEF4	Deformed	6400	3400	8.28
HOK4	Hooked	7460	4500	10.80

* Fiber content = 4% by volume

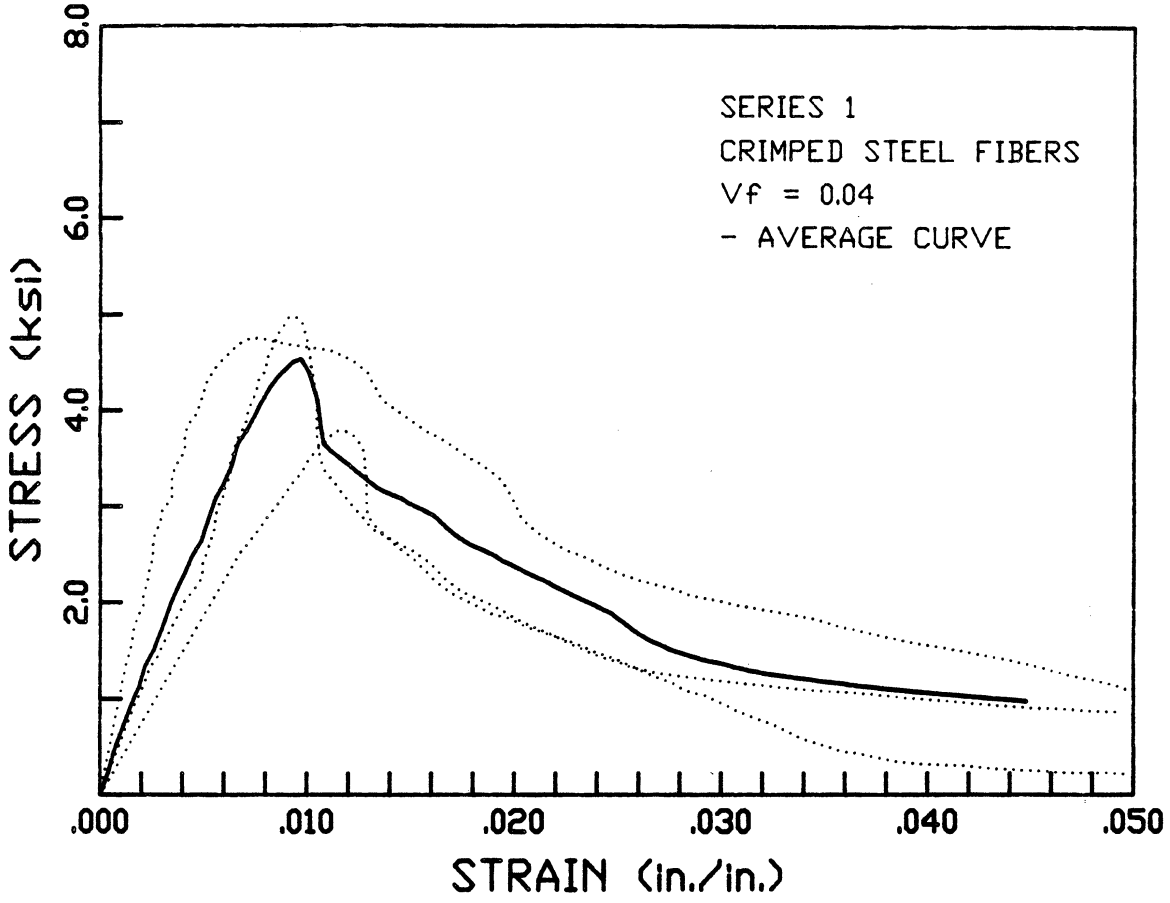

Fig. 3.4- Stress-strain curve for cylinders containing crimped steel fibers.

decreasing beyond its maximum value to an asymptotic stress value of 900 psi at 5% strain. The toughness index was 3.75.

Polypropelene Plastic Fibers in Mortar Matrix: (l=3/4 in, V_f=4 %)

The stress-strain curve for the specimens containing polypropelene fibers is shown in Fig.3.5. The addition of the fibers increased the average maximum compressive stress to 5670 psi. The compression stiffness was also increased. However, the toughness index was 3.14, the smallest observed among the specimens of the first series. The asymptotic stress at 5% strain was also the smallest at 560 psi.

Flat Steel Fibers in Mortar Matrix: (l=3/4 in, V_f=4 %)

As shown in Fig.3.6, the addition of flat steel fibers to the mortar mix produced a stiffer, stronger, and tougher matrix. The average maximum compressive stress obtained was 6400 psi, and the asymptotic stress value at 5% strain was 1100 psi. The toughness index was 5.41.

Deformed Steel Fibers in Mortar Matrix: (l=30 mm, V_f=4%)

As shown in Fig.3.7, a better overall behavior was observed for the specimens containing deformed steel fibers. An increase in the compression stiffness was reported along with an increase in the average maximum compressive stress up to 6400 psi. A shallow slope beyond the maximum compressive stress leading to an asymptotic stress of 3400 psi at 5% strain represented the specimen's significant toughness. The toughness index was 8.28.

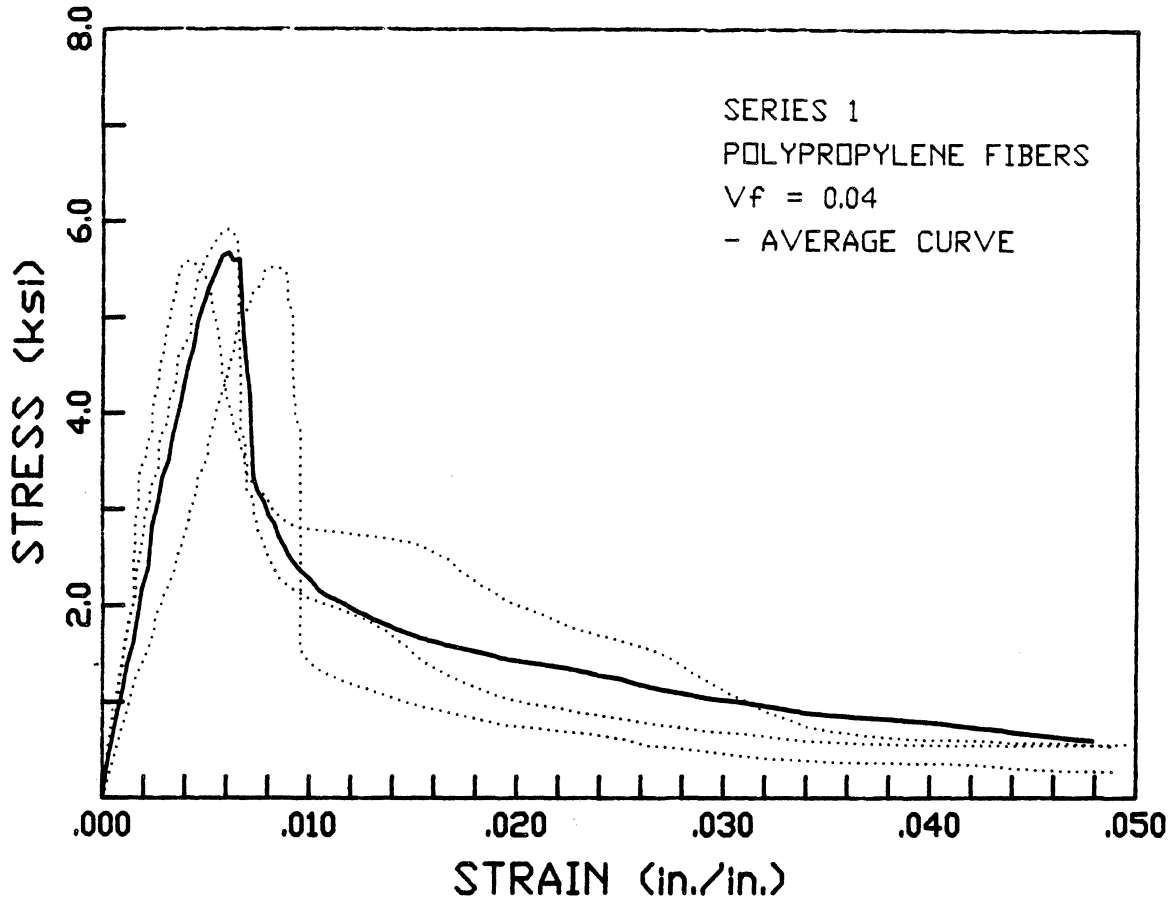

Fig. 3.5- Stress-strain curve for cylinders containing polypropelene plastic fibers.

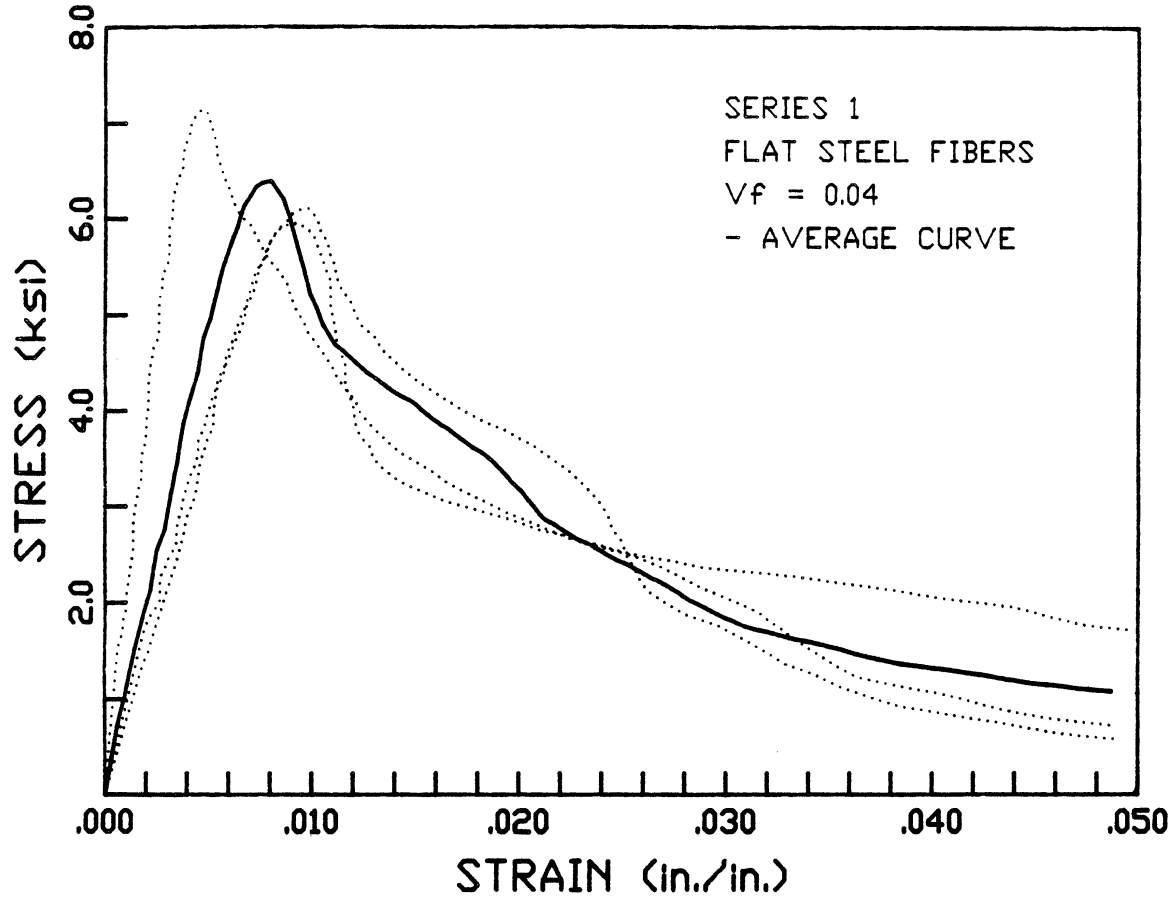

Fig. 3.6- Stress-strain curve for cylinders containing flat steel fibers.

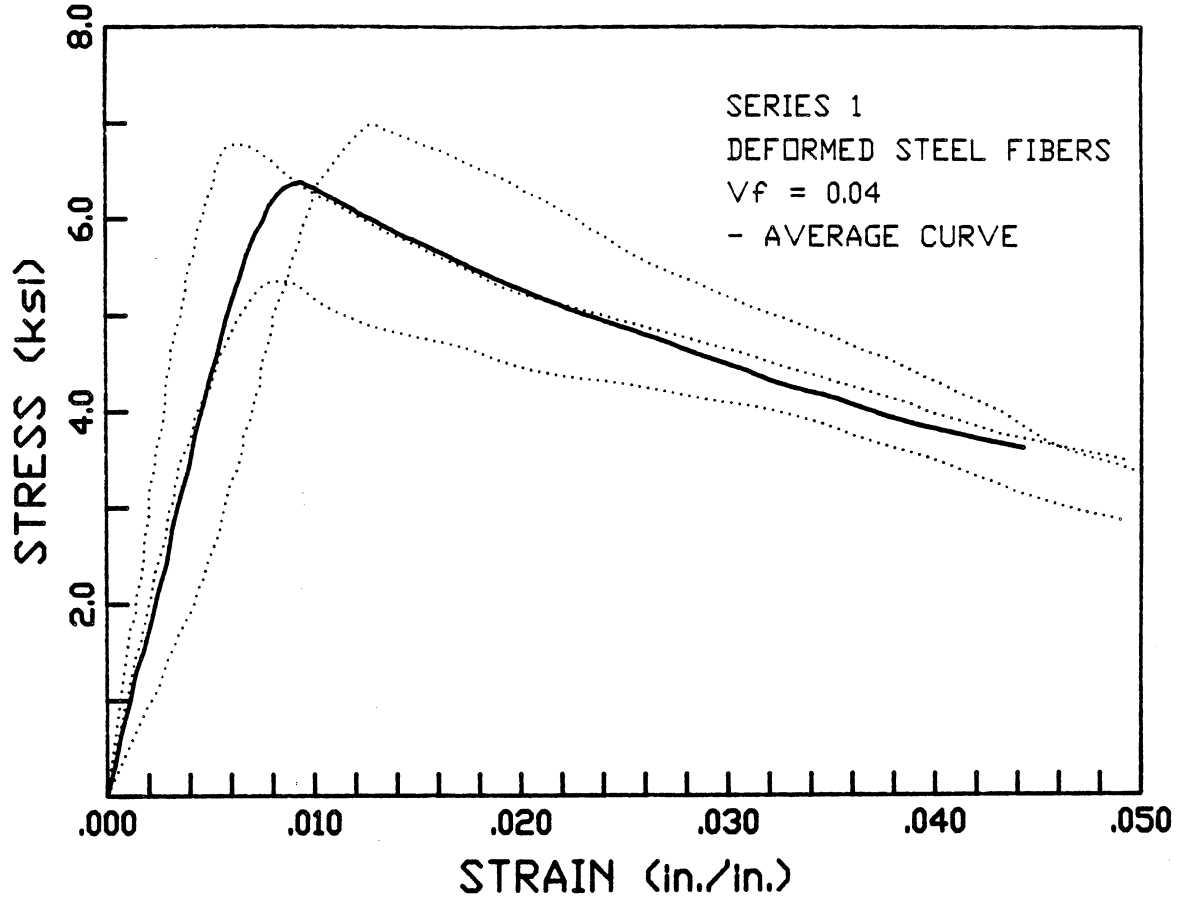

Fig. 3.7- Stress-strain curve for cylinders containing deformed steel fibers.

Hooked Steel Fibers in Mortar Matrix: (l=30 mm, Vf=4%)

The stress-strain curve for the specimens containing hooked steel fibers is shown in Fig.3.8. These specimens exhibited the best behavior of the first series. The average maximum compressive stress was 7460 psi and the toughness was represented by a very small descending branch slope, producing an asymptotic stress of 4500 psi at 5% strain. The toughness index was 10.8.

Based on the compressive behavior of the cylinders it was decided that the specimens containing hooked and deformed steel fibers were adequate for use in the CIP joints of the beam-type specimens. The specimen containing polypropelene plastic fibers was also selected since it exhibited the best mixing workability. Another reason for this selection was the interest in observing the behavior of a plastic fiber composite under cyclic loading.

3.4 -Series II Characteristics

3.4.1 -Mix Design

Difficulties were encountered in the casting of the chosen steel FRC composites from the Series I cylinders specimens in the joints of the beam type specimens. This necessitated the design and testing of Series II cylinders specimens. The difficulties were the segregation of the mix during the casting process and the absence of adequate vibration. Segregation occurred because, unlike the open cylinders where the FRC composite was originally cast, the joint area was somewhat congested with reinforcement extending from the two parts of the precast beam.

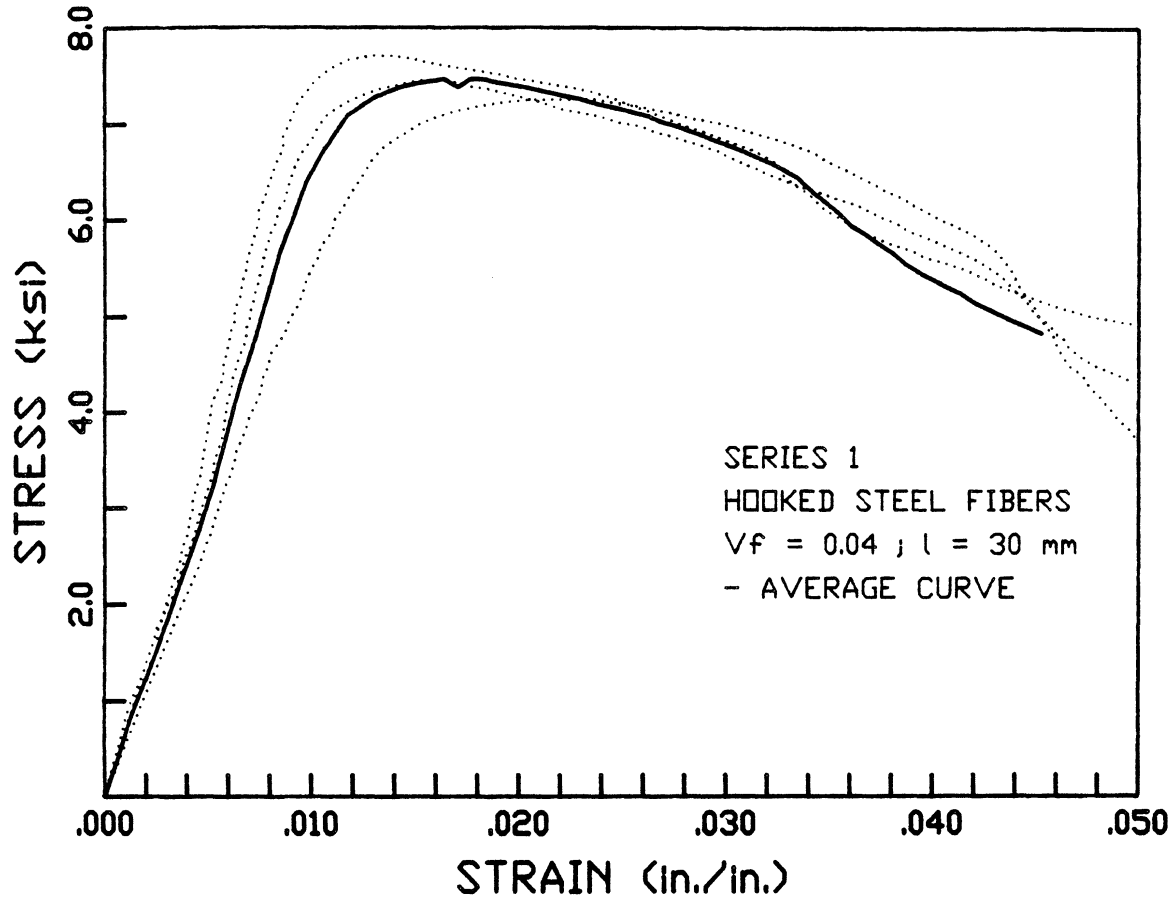

Fig. 3.8- Stress-strain curve for cylinders containing hooked steel fibers.

Therefore, when the FRC composite was gradually cast in the joint area, only the mortar mix penetrated the gaps between the reinforcing bars, leaving out the fibers and causing segregation of the mix. Moreover, the available vibrator was used on the outside of the mold to simulate the external vibration used in casting the cylinders, and this led to further segregation of the mix.

Therefore, despite good mixing workability, the poor casting workability of the FRC composites prompted the design of somewhat denser FRC composites to provide a better casting workability. A pastier mix was obtained by adding an additional part of sand to the mortar mix. The mortar mix in Series II, therefore, contained two parts of sand instead of only one, as was used in Series I. The addition of a part of sand to the mortar mix produced, as expected, a denser and more workable steel FRC composite although a reduction in the maximum compression strength was anticipated.

3.4.2 -Test Results

The test results of Series II are summarized in Table 3.4. The control specimens failed in a brittle manner, providing an average maximum compressive strength of 4100 psi.

Deformed Steel Fibers in Mortar Matrix: (l=30 mm, V_f=4 %)

The stress-strain curve for the specimens containing deformed steel fibers is shown in Fig.3.9. The change in the mortar mix did not significantly affect its stiffness. The average maximum compressive

Table 3.4- Series II test results.

Name	Fibers * in Cylinder	Maximum Comp. Stress *(psi)*	Asymptotic Stress *(psi)*	Toughness Index
CONTROL II	---	4100	0	1.00
HOK4	Hooked	6200	3000	8.18
DEF4	Deformed	6670	2800	8.03

* Fiber content = 4% by volume

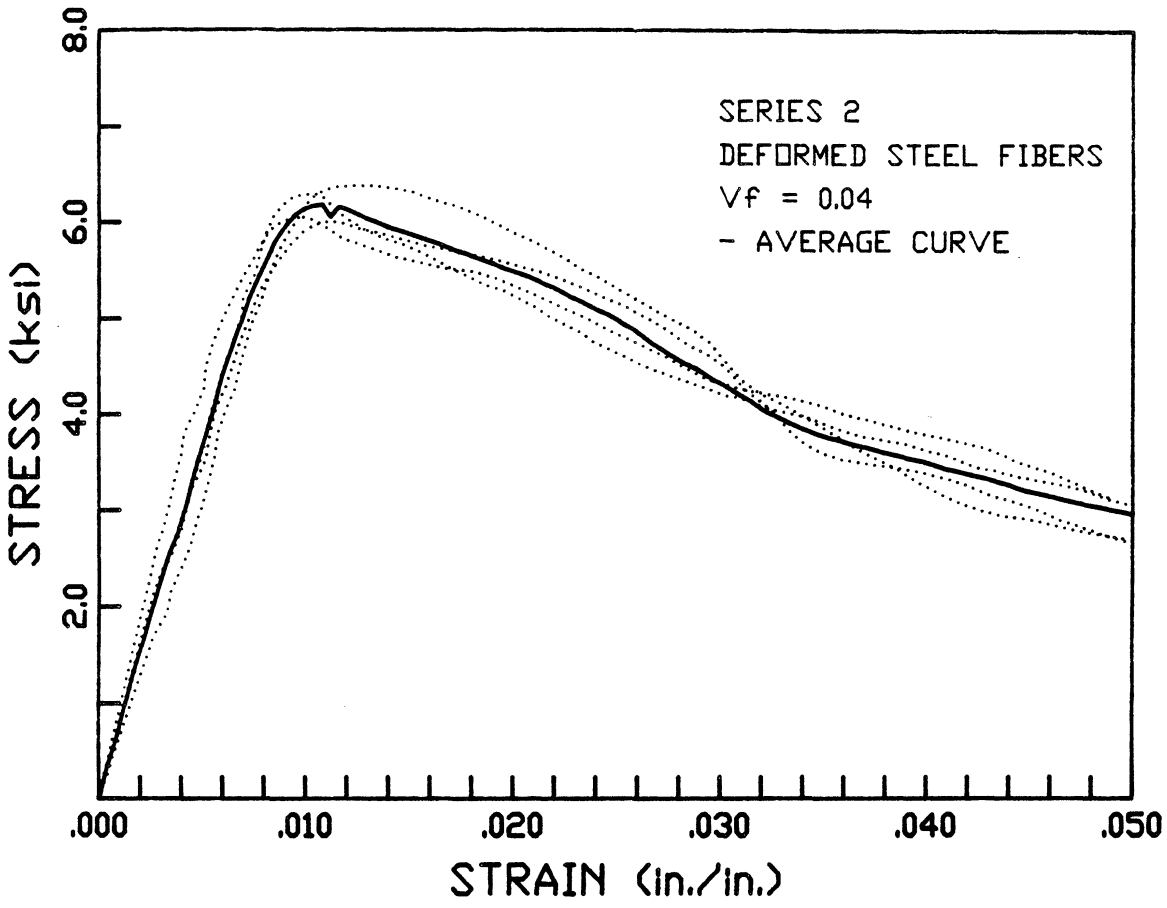

Fig. 3.9- Stress-strain curve for cylinders containing deformed steel fibers.

stress was 6200 psi. The asymptotic stress at 5% strain, compared to Series I, dropped to 3000 psi and the toughness index to 8.18.

Hooked Steel Fibers in Mortar Matrix: (l=30 mm, V_f=4 %)

The stress-strain curve for the specimens containing hooked steel fibers is shown in Fig.3.10. Here also, the change in the FRC matrix mortar mix did not significantly affect the matrix stiffness. The average maximum compressive stress was 6670 psi. However, the asymptotic stress at 5% strain, compared to Series I, dropped to 2800 psi, and the toughness index to 8.03. As anticipated, the addition of a part of sand to the mortar mix affected the compressive behavior of the composites. The composite containing deformed steel fibers was only slightly affected whereas the composite containing hooked steel fibers was more significantly affected. The primary goal, however, which was obtaining a better casting workability for the composite, was achieved.

3.5 -Series III Characteristics

3.5.1 -Mix Design

In the third series of cylinder tests, the concrete mix contained aggregate in addition to cement and sand. In addition to the hooked and deformed fibers which were the same fibers used in the two previous series (l = 30 mm & l/d = 60), longer hooked fibers were also used (l = 50 mm & l/d = 100). The fiber volume fraction was 2.1% for the 30 mm hooked and deformed fibers, and 1% for the 50 mm hooked fibers. The reduction in the fiber volume fraction was due to the presence of the coarse aggregate which made mixing more difficult even in the absence of

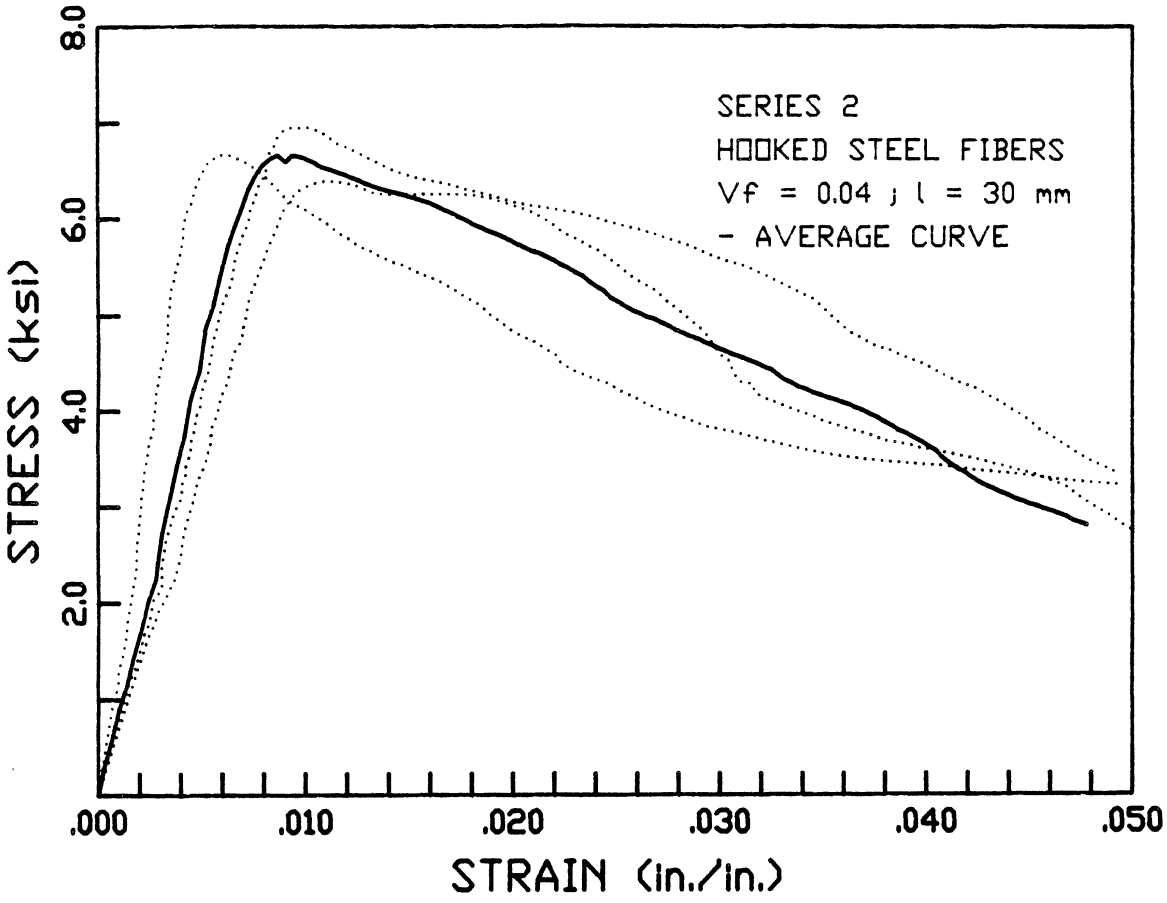

Fig. 3.10- Stress-strain curve for cylinders containing hooked steel fibers.

fibers. In general, when fibers are added to a concrete mix the workability is significantly reduced and consequently the fiber volume fraction must be reduced to maintain adequate workability. In the case of the 50 mm hooked steel fibers, the problem was further complicated since the aspect ratio, l/d, of the fibers was almost doubled. Thus, the fiber volume fraction was further reduced.

The concrete composites were tested along with the mortar composites that were to be used in the CIP joints, i.e., the polypropelene composite specimen from Series I, as well as the hooked and deformed composites specimens from Series II. It was believed that the testing of all the composites in one series, would provide a good basis of comparison since the specimens were cast, cured, and tested under the same conditions. Furthermore, when collecting the test data, three LVDTs (linear variable differential transformers) were used to measure the movement of the plattens of the testing machine instead of the single LVDT housed inside the actuator.

3.5.2 -Test Results

The test results of Series III are summarized in Table 3.5. The concrete control specimens failed in a brittle manner, providing an average maximum compressive strength of 5580 psi.

Deformed Steel Fibers in Concrete Matrix: (l=30 mm, V_f=2.1 %)

The stress-strain curve is shown in Fig.3.11. The addition of fibers to the mix increased the average maximum compressive stress to 8900 psi. This addition of fibers, however, did not have a significant effect on the

Table 3.5- Series III test results.

Name	Fibers in Cylinder	Matrix	Vol. Fraction	Modulus of Elasticity *(ksi)*	Maximum Comp. Stress *(psi)*	Asymptotic Stress *(psi)*	Toughness Index
CONTROL I	---	Mortar	---	---	4200	0	1.00
POLY4	Polypropelene	Mortar	4%	2010	4700	760	2.90
CONTROL II	---	Mortar	---	---	4100	0	1.00
DEF4	Deformed	Mortar	4%	3350	7730	2100	6.28
HOK4	Hooked	Mortar	4%	3650	8200	1850	7.08
CONTROL III	---	Concrete	---	---	5580	0	1.00
DEF2.1	Deformed	Concrete	2.1 %	4370	8900	270	4.50
HOK2.1	Hooked	Concrete	2.1 %	4000	8300	2100	4.87
HOK1	Hooked *	Concrete	2.1 %	5500	8700	390	3.89

* Fiber length = 50 mm

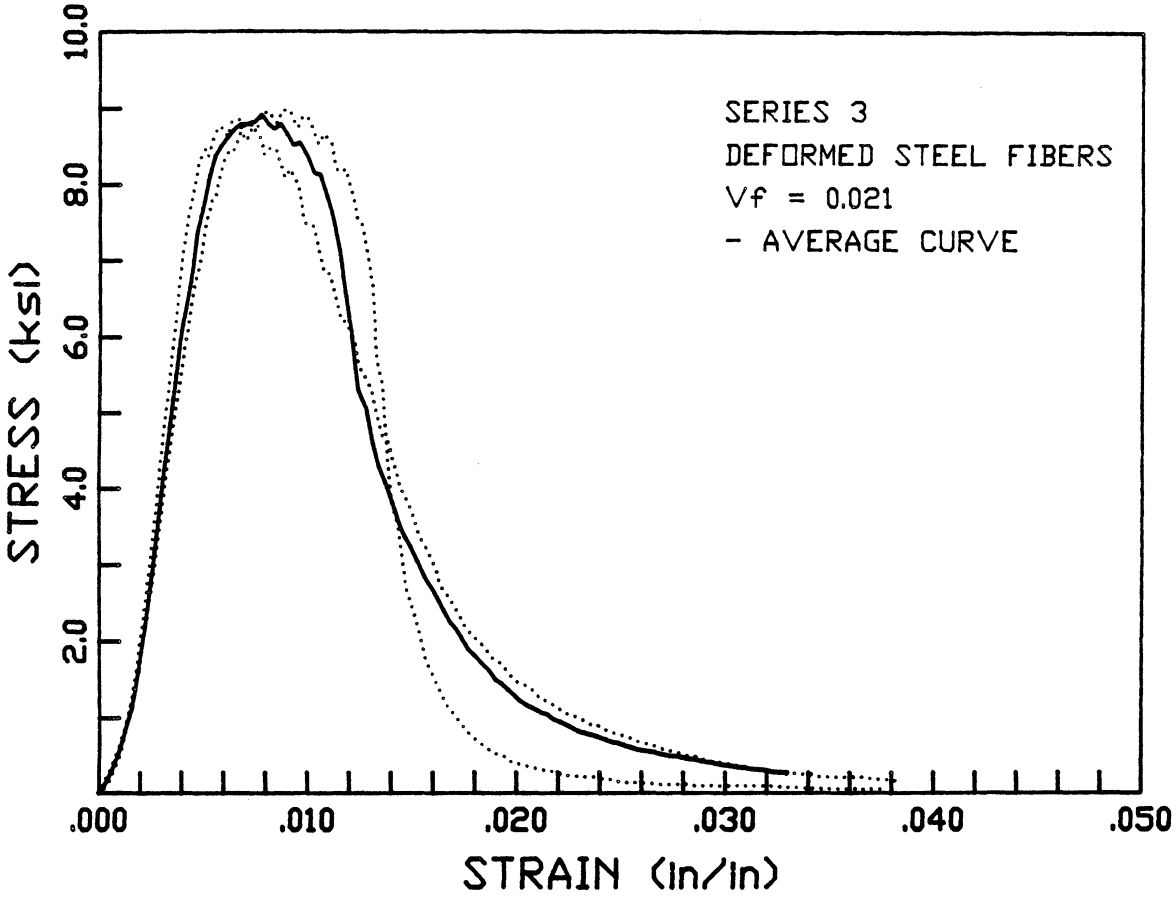

Fig. 3.11- Stress-strain curve for cylinders containing deformed steel fibers.

descending branch of the stress-strain curve. The stress beyond the peak rapidly decreased to an asymptotic value of 270 psi, providing, therefore, a relatively low toughness index of 4.50. The modulus of elasticity was 4370 ksi.

Hooked Steel Fibers in Concrete Matrix: (l=30 mm, V_f=2.1 %)

The stress-strain curve is shown in Fig.3.12. Due to the addition of fibers, the average maximum compressive stress increased to 8300 psi. A high post peak slope was also observed. The asymptotic stress was 2100 psi, which was larger than that observed for deformed fibers. The toughness index was 4.87, and the modulus of elasticity was 4000 ksi.

Hooked Steel Fibers in Concrete Matrix: (l=50 mm, V_f=1 %)

The stress-strain curve is shown in Fig.3.13. An average maximum compressive stress of 8700 psi was observed, along with a high post peak slope leading to a small asymptotic stress of 390 psi, and a toughness index of 3.89. The modulus of elasticity was 5500 ksi.

For the specimens selected from Series I and II, i.e, polypropelene, hooked, and deformed fibers added to mortar matrices, the overall behavior of these specimens was similar to those tested in Series I and II. However, the average maximum compressive stresses observed were higher. This was related to the fact that the specimens from Series III were tested 9 months after casting, whereas the specimens from Series I and II were tested only 28 days after casting. The differences observed in the modulus of elasticity were due to the fact that in Series III the platten movement was measured more accurately.

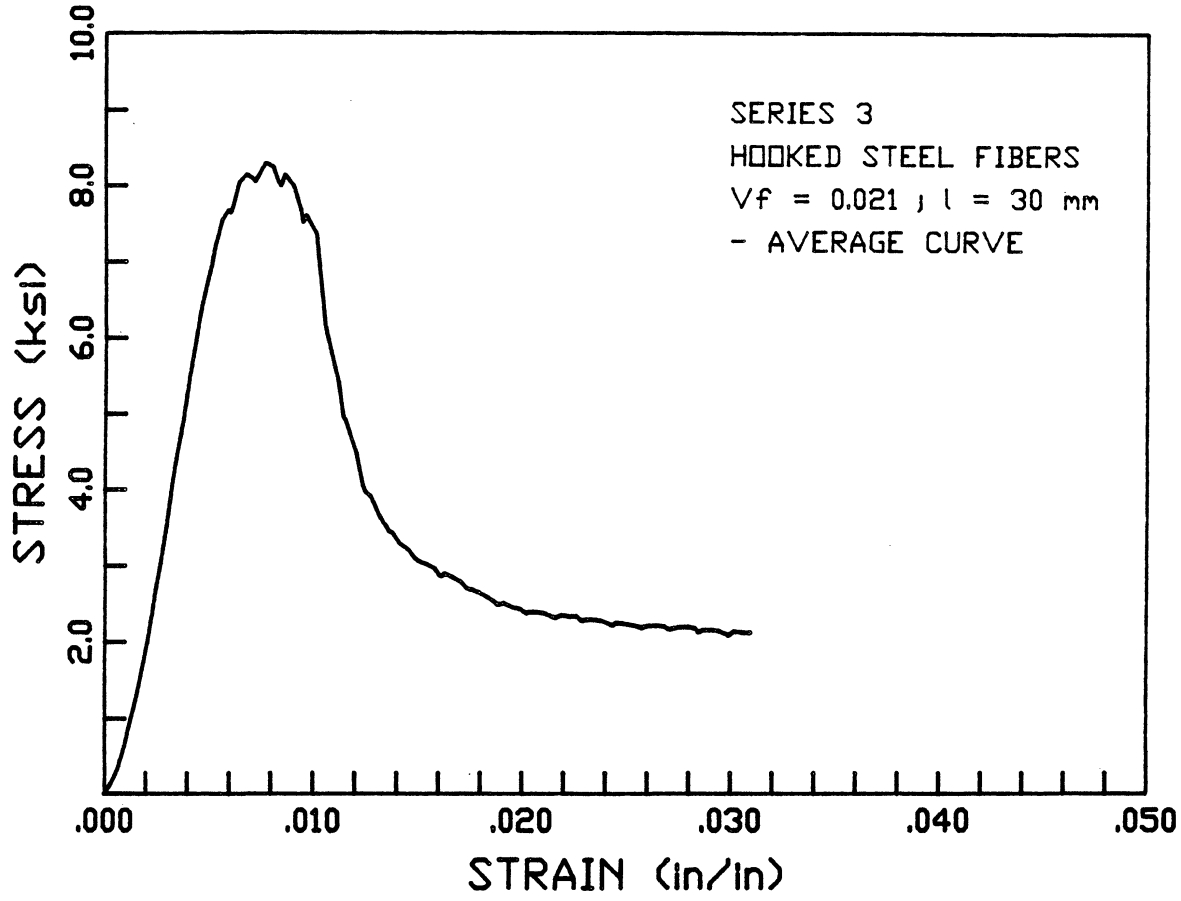

Fig. 3.12- Stress-strain curve for cylinders containing hooked steel fibers.

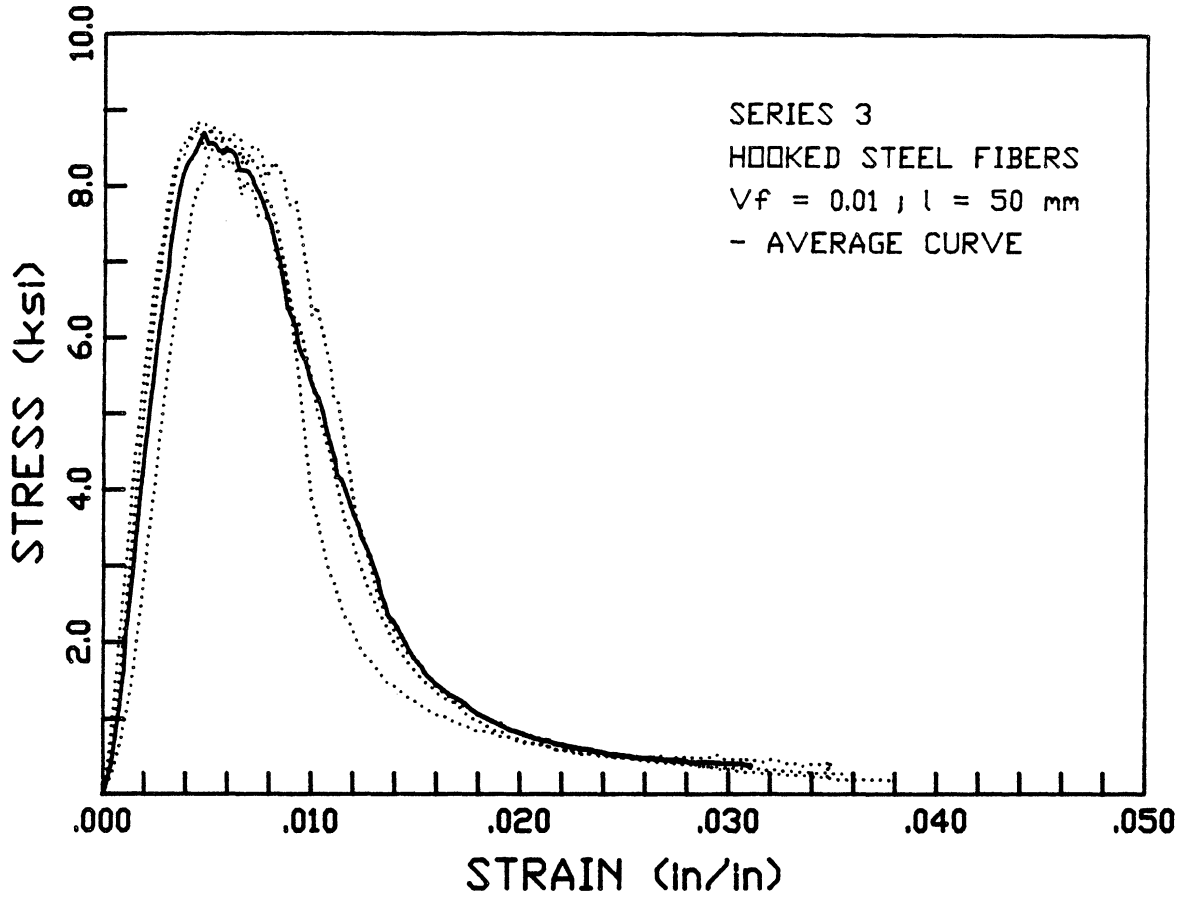

Fig. 3.13- Stress-strain curve for cylinders containing hooked steel fibers.

Polypropelene Plastic Fibers in Mortar Matrix: (l=3/4 in, V_f=4 %)

The stress-strain curve is shown in Fig.3.14. The average maximum compressive stress was 4700 psi. The asymptotic stress was 760 psi, and the toughness index was 2.9. The modulus of elasticity was 2010 ksi.

Deformed Steel Fibers in Mortar Matrix: (l=30 mm, V_f=4 %)

The stress-strain curve is shown in Fig.3.15. The average maximum compressive stress was 7730 psi. The asymptotic stress was 2100 psi, and the toughness index was 6.28. The modulus of elasticity was 3350 ksi.

Hooked Steel Fibers in Mortar Matrix: (l=30 mm, V_f=4 %)

The stress-strain curve is shown in Fig.3.16. The average maximum compressive stress was 8200 psi. The asymptotic stress was 1850 psi, and the toughness index was 7.08. The modulus of elasticity was 3650 ksi.

Based on the test results, the composites in this series were considered adequate to be placed in the CIP joints of the beam specimens. The behavior of those specimens is discussed next in Chapter 4.

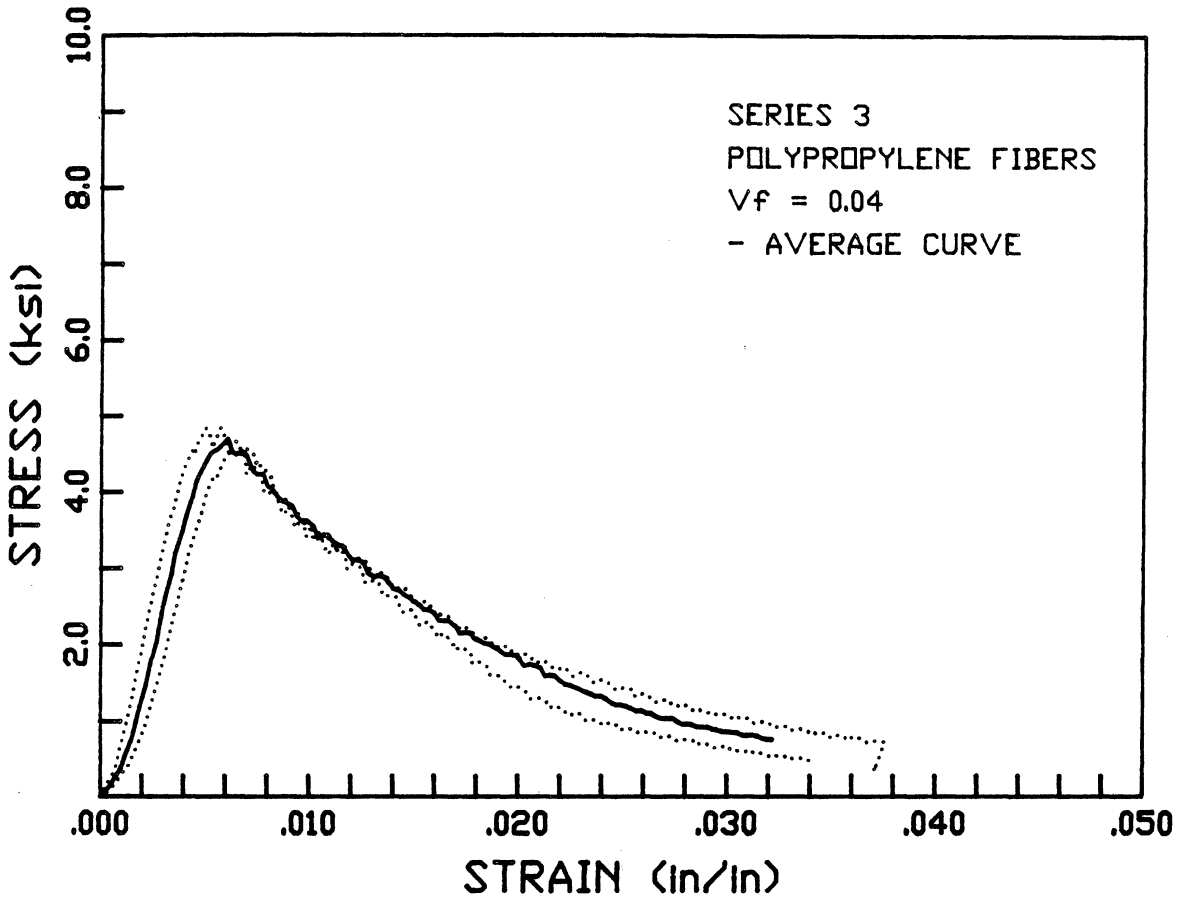

Fig. 3.14- Stress-strain curve for cylinders containing polypropelene plastic fibers.

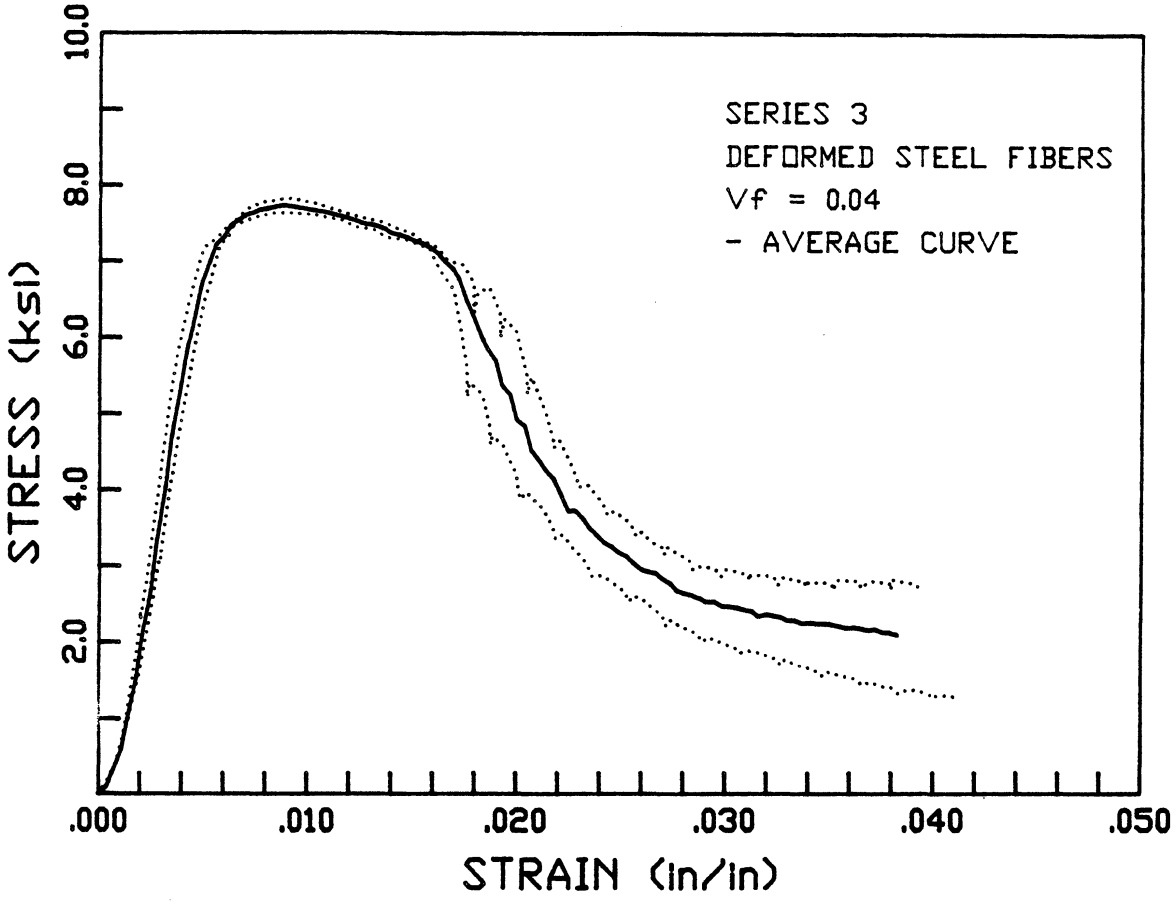

Fig. 3.15- Stress-strain curve for cylinders containing deformed steel fibers.

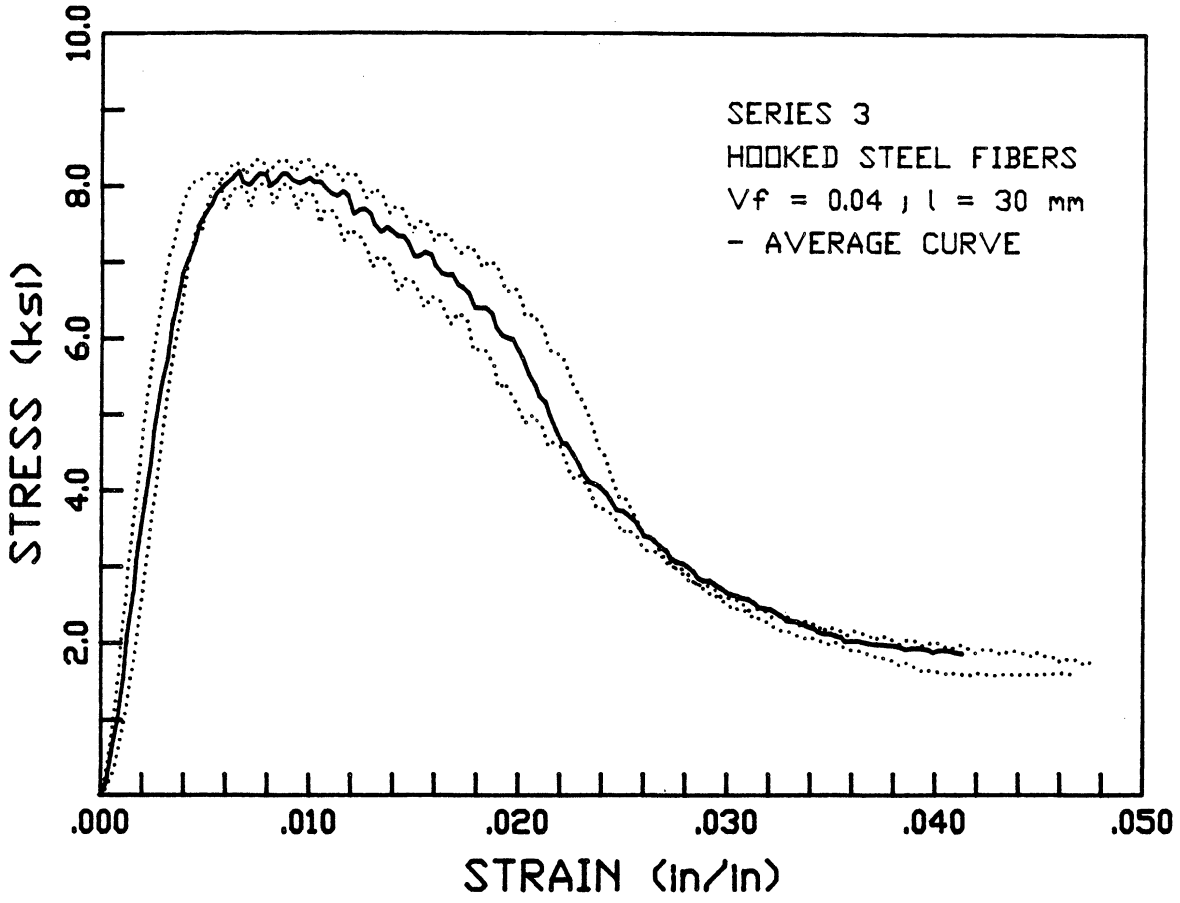

Fig. 3.16- Stress-strain curve for cylinders containing hooked steel fibers.

CHAPTER IV

EXPERIMENTAL PROGRAM

PART II : BEAMS TESTS

4.1 -Design of Beam Specimens

This part of the investigation consisted, as mentioned earlier, of the testing of six beam-type specimens. A typical beam-type specimen is shown in Fig.3.1. Each specimen consisted of two reinforced concrete precast parts joined together by a cast-in-place (CIP) fiber reinforced concrete (FRC) joint. The characteristics of the individual specimens are summarized in Table 4.1. The steel configuration used is shown in Fig.4.1. This configuration provided 3 No. 4 + 2 No. 3 bars outside the CIP joint and 4 No. 3 bars inside the CIP joint. This configuration was previously used by Abdou (1) in a similar investigation where slurry infiltrated concrete (SIFCON) was used as the CIP joint material. The arrangement of the bars extending into the joint provided adequate anchorage and, therefore, prevented slippage of the bars.

Table 4.1- Beam specimens characteritics.

Specimen	Matrix	Series	Properties of Fibers in the CIP joint		
			Name	*Length*	*Volume Fraction*
POLYCS4	Mortar	I	Polypropelene	3/4 in.	4.00%
H30C2S4	Mortar	II	Hooked	30 mm	4.00%
D30C2S4	Mortar	II	Deformed	30 mm	4.00%
H30CON2.1	Concrete	III	Hooked	30 mm	2.10%
D30CON2.1	Concrete	III	Deformed	30 mm	2.10%
H50CON1	Concrete	III	Hooked	50 mm	1.00%

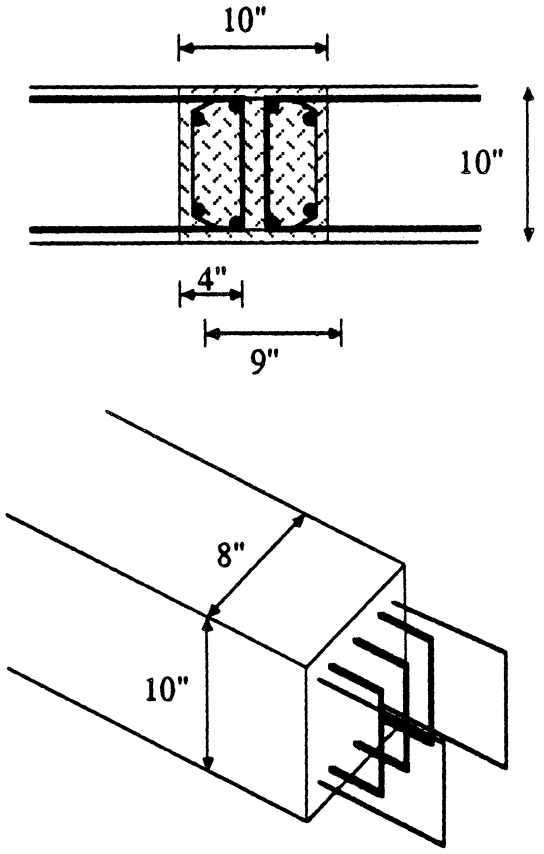

Fig. 4.1- Steel configuration in specimen.

4.1.1 -Material Properties

The precast portions of the beam specimens were designed to have a 28-day concrete strength of 6000 psi. Concrete for the precast portions was obtained from a local concrete plant. The concrete mix was designed using Type I Portland Cement and a well graded gravel with 3/8 inch maximum aggregate size. The water to cement ratio was selected to produce a workable mix and to facilitate compaction. All the segments were cast from one batch, from which eighteen 4 in. x 8 in. cylinders were cast to determine the concrete compressive strength at 28 days and at the time the specimens were tested.

Grade 60 No. 3, and No. 4 bars were used as the beam main reinforcement. The beam stirrups were formed from 3/16 in. diameter bars. The properties of the reinforcing steel and concrete are given in Table 4.2.

4.1.2 -Fabrication of Specimens

Prior to casting the beam segments, the wooden forms were oiled on their interior surface to facilitate disassembly after the concrete hardening. The forms were also sealed on the exterior surface to prevent concrete leakage during casting. Strain gages were placed at appropriate locations on the reinforcing bars. The rebar cages were placed in the oiled forms of the precast elements with the rebars to be used in the CIP joint protruding from one end. Concrete was then poured from a ready mix truck. A hand held vibrator was used to ensure concrete compaction.

Bar Size	Grade	Yield Stress *fy (ksi)*	Ultimate Stress *fsu (ksi)*
# 3/16	---	79	---
# 3	60	65.5	106
# 4	60	76.3	104.8

Table 4.2- a) Properties of reinforcing steel.

Specimen #	f'c *(psi)*
1	7520
2	6680
3	7640
4	8000
5	6450
6	6370

Table 4.2- b) Properties of concrete.

After hardening and curing of the concrete, the wooden forms were removed and the precast elements were brought together with the protruding steel from both elements overlapped to form the joint. These elements were placed on their side to facilitate the casting of the joint. Wooden forms were placed around the joint, oiled and sealed, and the joint composite was then cast. The different stages of assembly are shown in Fig.4.2.

4.2 -Test Setup

The testing setup is shown in Fig.4.3. The beam specimen is subjected to concentrated loads at the third points in both the upward and downward directions. The machine used was a Universal Testing Machine (Instron System 8000) with a 120 kip maximum hydraulic actuator capacity. A steel spreader beam was attached to the actuator load cell and loading pads were attached between the spreader and the beam test specimen at the desired loading points. The beam specimens had two hinge supports near its ends. A system of box steel beams and circular rods was fabricated and placed at the beam supports and the loading points to provide appropriate supports and loading points in the upward direction.

4.2.1 -Data Acquisition

Data was collected from four sources throughout the tests: (1) photographic record of the specimens, (2) load and displacement of the hydraulic actuator as well as displacement of transducers (LVDTs) placed

Fig. 4.2- a) Assembled steel cages.

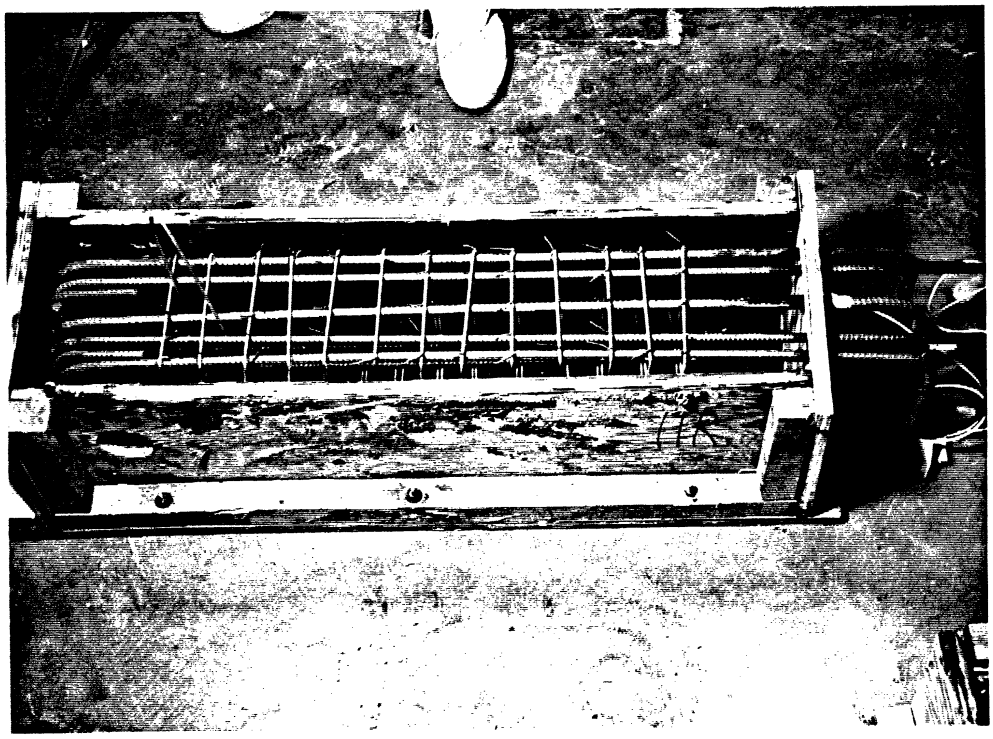

Fig. 4.2- b) Steel cages in molds.

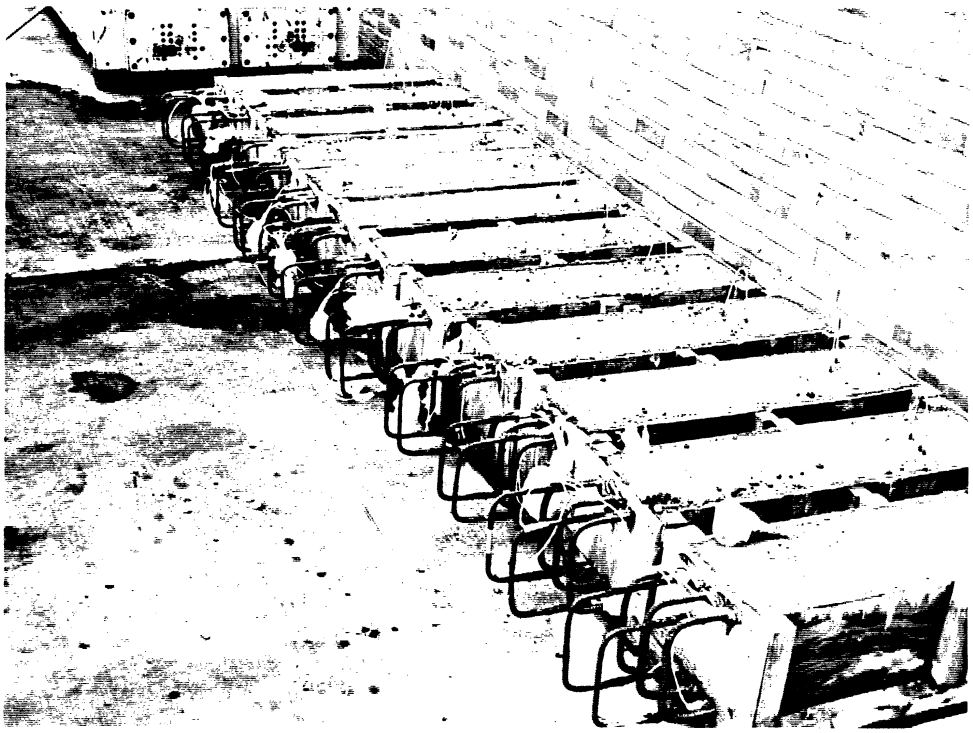

Fig. 4.2- c) Beam parts after casting.

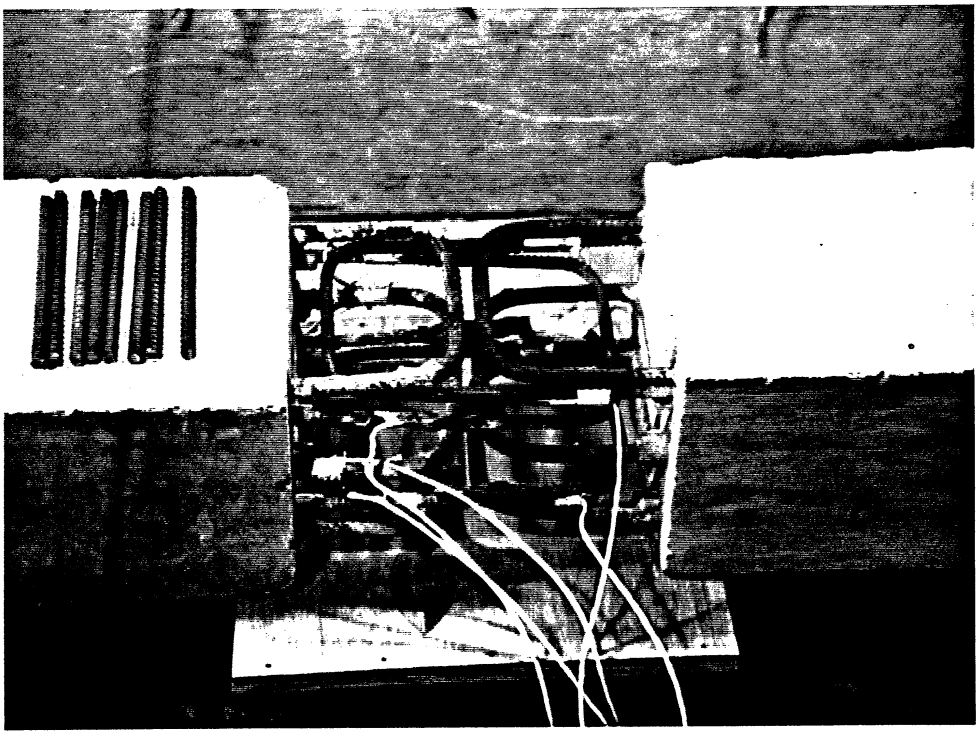

Fig. 4.2- d) Joining precast parts.

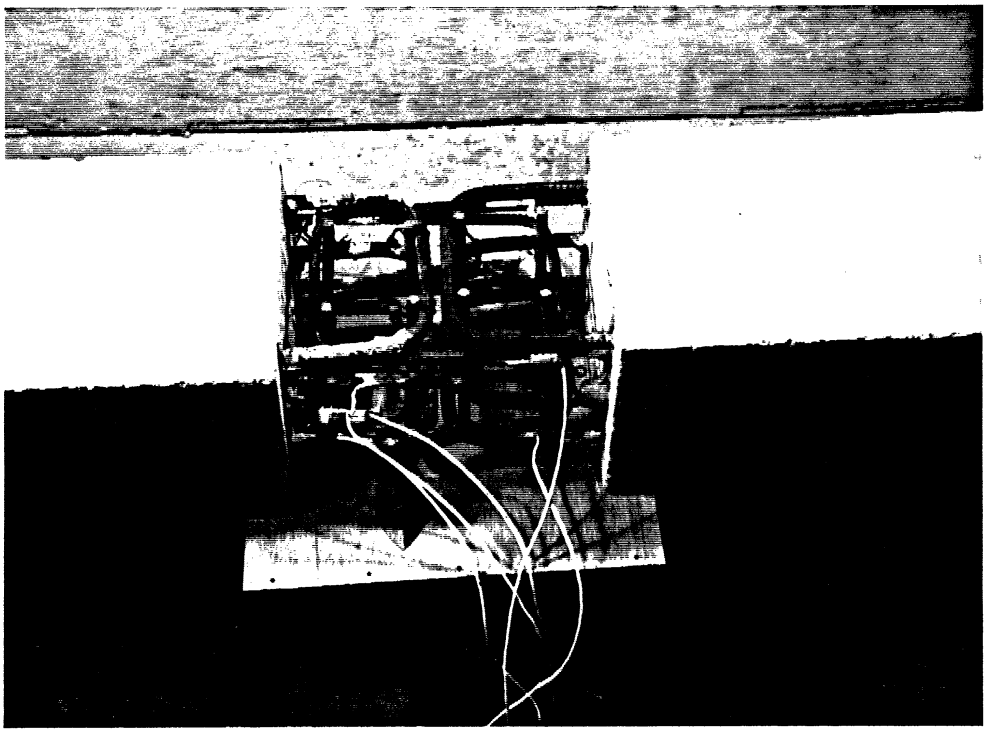

Fig. 4.2- e) Steel arrangement in joint area.

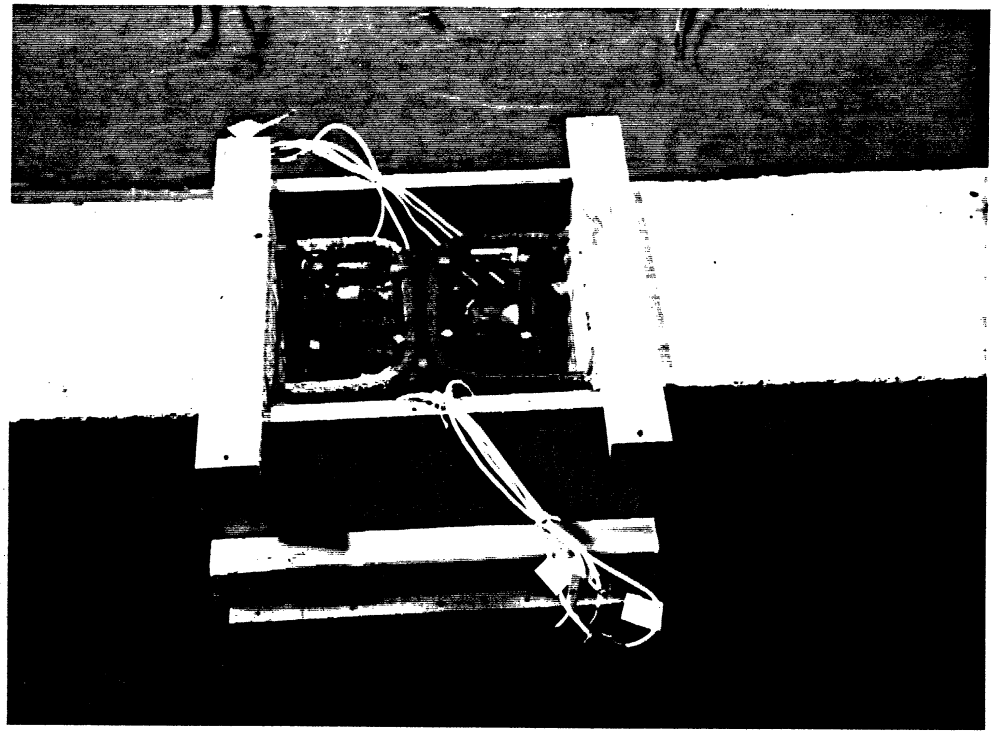

Fig. 4.2- f) CIP joint ready for casting.

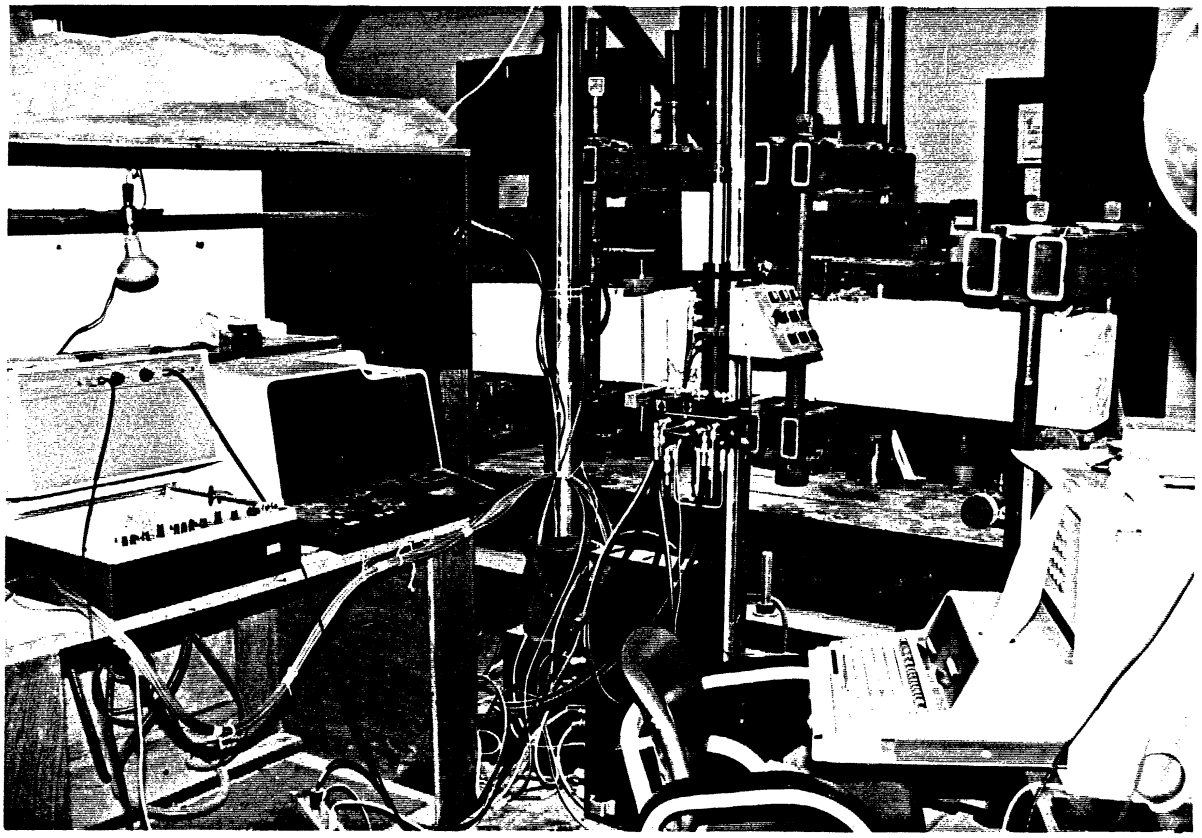

Fig. 4.3- Testing setup.

under the CIP joint, and (3) electrical resistance strain gages bonded to the reinforcing bars.

An x-y plotter was used to obtain a continuous plot of the load vs. displacement of the hydraulic actuator. The plots were used to determine the yield displacement as well as to monitor the specimen behavior throughout the test.

The strains in the reinforcing steel were measured through a set of strain gages bonded to the reinforcement inside and outside the CIP joint. Each specimen had twelve strain gages. Fig.4.4 shows the location of those gages for one portion of the test beams.

4.2.2 -Loading Sequence

All the tests were controlled by the actuator displacements. The loading history is shown in Fig.4.5. This loading history was used since it was found in previous studies to provide sufficient information on the strength as well as the stiffness degradation of the specimen. The displacement of the specimen at yield served as a guideline in defining the specimen ductility in subsequent cycles.

4 = No. 4 Bar
3 = No. 3 Bar
R = Right Half
L = Left Half
T = Top Bar
B = Bottom Bar

I = Inside the Joint
O = Outside The Joint
-B = Back
-F = Front

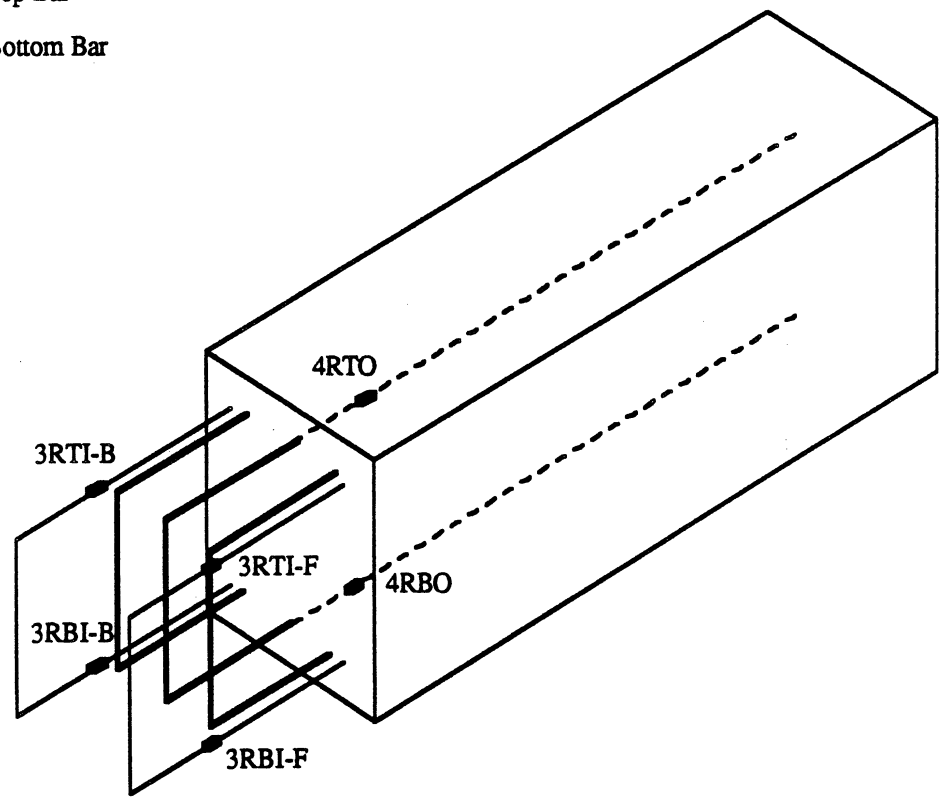

Fig. 4.4- Strain gages location.

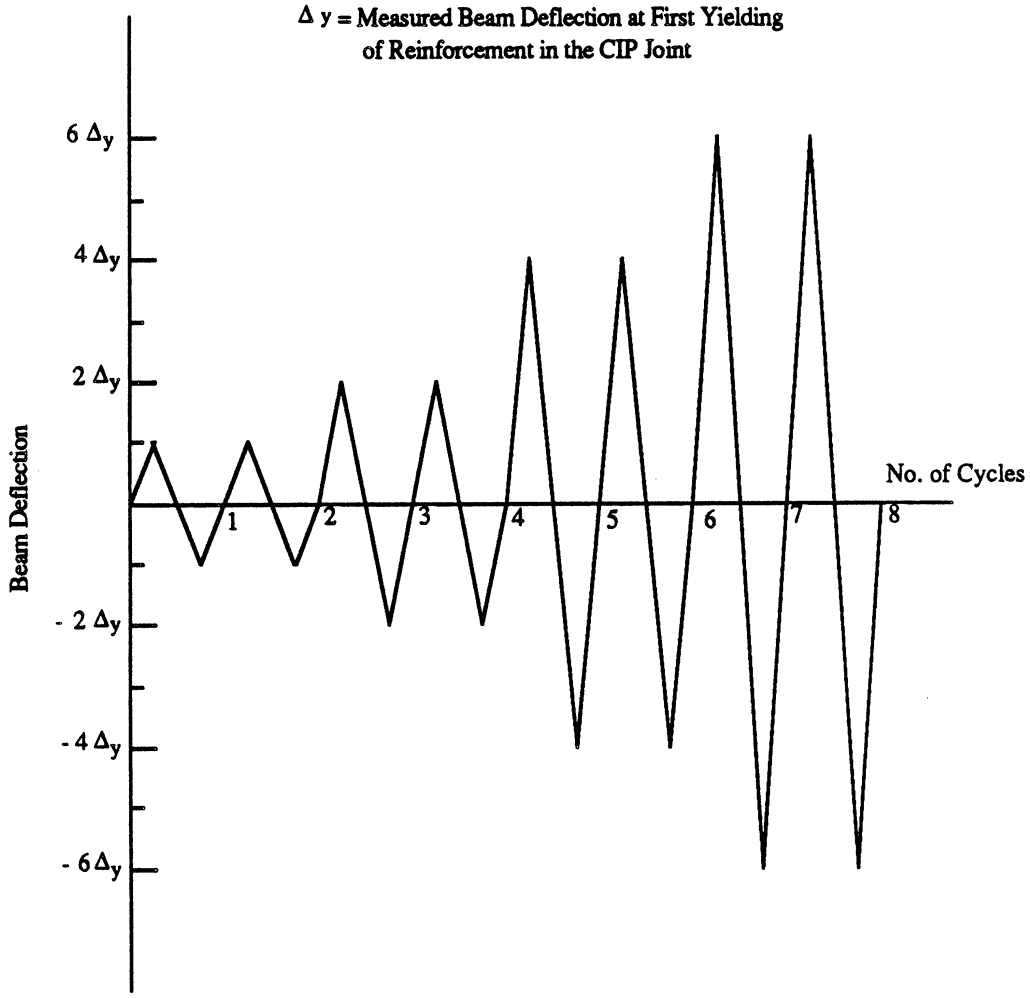

Fig. 4.5- Loading history.

4.3 -Test Results

The overall behavior of each specimen was analysed using the following sources of information:

1- Photographic records of the specimens

This record was used to monitor the development and growth of cracks in the specimens. The photographs were taken at the end of each half cycle, after marking the crack pattern.

Several flexural cracks formed in the CIP joint as soon as the specimens were loaded. Flexural cracks also appeared along the interfaces between the precast segments and the CIP joint. In addition to the flexural cracks, shear cracks also appeared in the beams. However, as the test progressed, one major flexural crack in the middle of the joint continued to widen.

2- Load vs. displacement curves

As mentioned earlier, the specimens were tested acording to the loading history shown in Fig.4.5. The load was obtained from the load cell of the testing machine, and the displacements were obtained from the displacement transducers placed under the CIP joint. The load vs. displacement curves were used to monitor the stiffness, the load carrying capacity, and the energy dissipation of the specimens.

3- Strain gages data

Data from the strain gages, which were bonded to the reinforcement, inside and outside the CIP joint, was used to confirm the yield displacements for the specimens, and to detect any slippage in the beam bars.

4.3.1 -Individual Specimen Behavior

The beam specimens were named according to the type of the CIP composite in the joint area.

- The first part of the specimen's name indicates the type of fibers used: POLY for polypropelene fibers of 3/4 in length, H30 for hooked fibers of 30 mm length, H50 for hooked fibers of 50 mm length, and D30 for deformed fibers of 30 mm length.

- The second part indicates the type of the matrix: CS for a mortar matrix containing one part cement and one part sand, C2S for a mortar matrix containing one part cement and two parts sand, and CON for a concrete matrix.

- The third part indicates the fiber volume fraction used in the CIP composite: 4 for V_f=4%, 2.1 for V_f=2.1%, and 1 for V_f=1%.

Therefore, POLYCS4 is the specimen in which the CIP composite contains polypropelene fibers in a mortar mix, with a fiber volume fraction of 4%.

Specimen POLYCS4:

Three flexural cracks appeared in the middle of the joint area during the first cycle. Cracks also appeared at the interfaces. A single crack, located in the middle of the CIP joint, continued to widen as the test progressed, while the rest of the cracks ceased to widen. Shear cracks were also observed in the precast beam parts. Failure occurred in the middle of the CIP joint in the downward loading portion of cycle 8. This failure was due to the tension rupture of one reinforcing bar at a

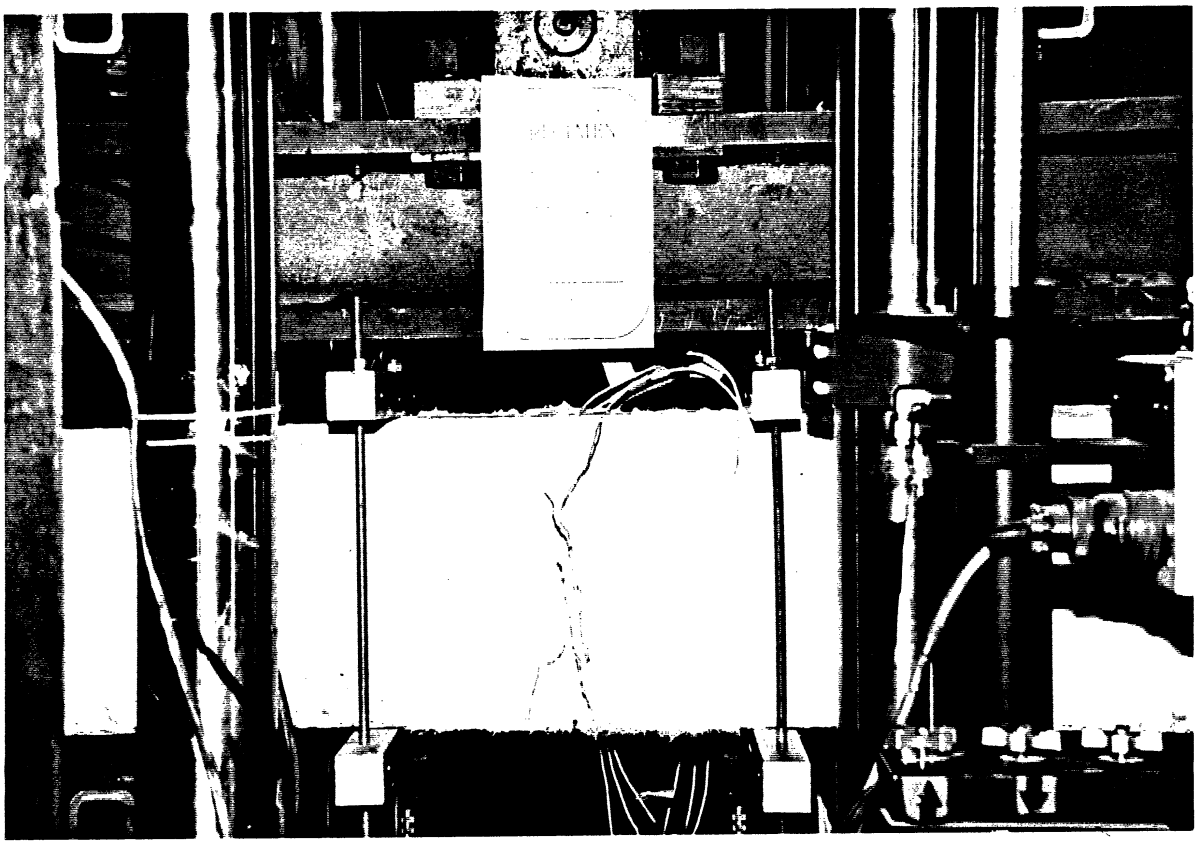

Fig. 4.6- a) Specimen at first cycle.

Fig. 4.6- b) Specimen at failure.

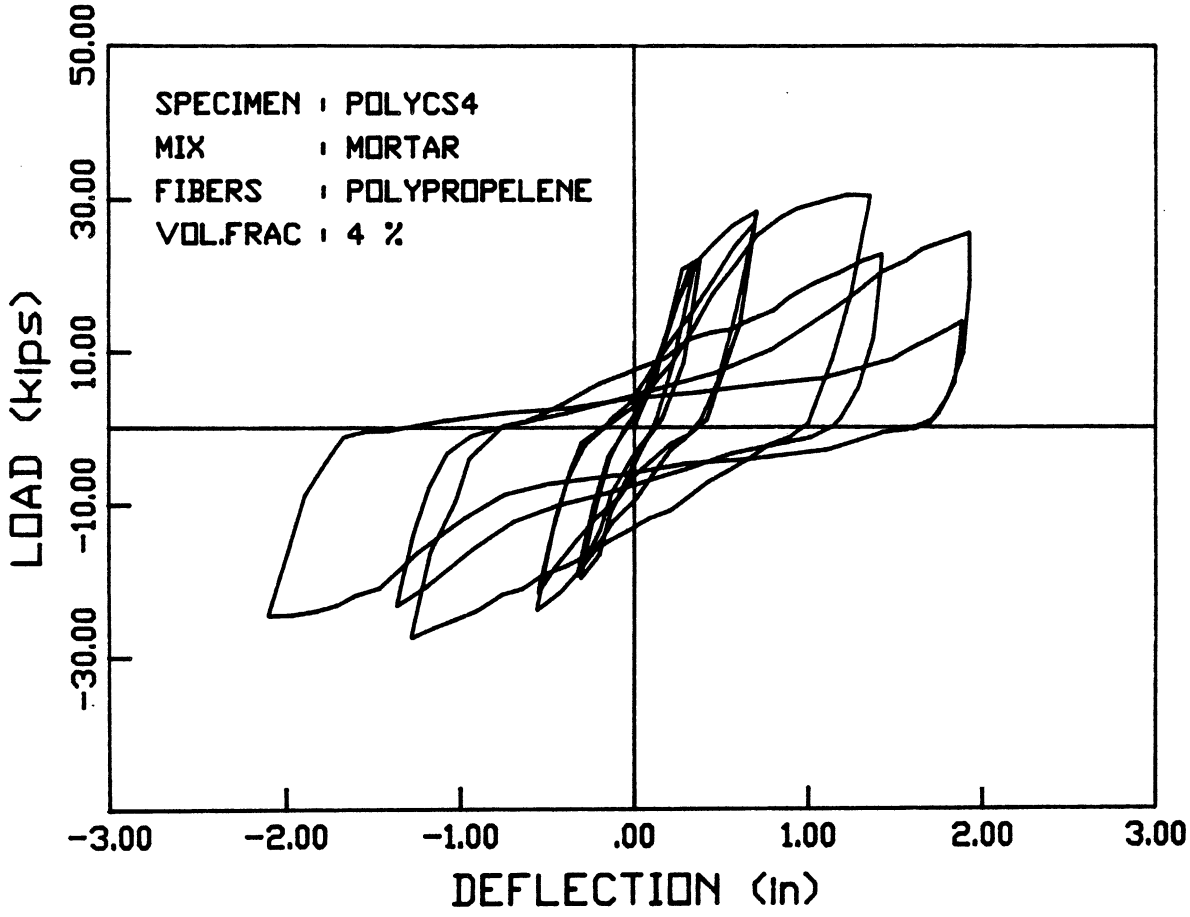

Fig. 4.7- Load vs. deflection curve.

displacement ductility of 5.8. Fig.4.6 shows the specimen at the first loading cycle and at failure. No slippage of the reinforcing bars occurred.

The load vs. deflection curve for this specimen is shown in Fig.4.7. The load carrying capacity decreased significantly in the 6th cycle. A loss of stiffness and pinching in the hysteresis loop was observed in that repeat cycle to a displacement ductility of 4.0.

Specimen H30C2S4:

During the first cycle of loading, the observed behavior was similar to that of the previous specimen. A few flexural cracks appeared inside the CIP joint as well as at the interface. Shear cracks also appeared in the precast beam parts. However, a single flexural crack continued to widen as the test progressed, whereas the other cracks ceased to do so. Failure occurred in the middle of the CIP joint after 5 loading cycles. This failure was caused by the tension rupture of two reinforcing bars inside the joint. The maximum displacement ductility in the 5th cycle was 3.3. Fig.4.8 shows the specimen in the second loading cycle and at failure. No slippage of the reinforcing bars occurred. This was verified after the test, when the concrete cover was stripped. A perfect imprint of the bars on the concrete was observed, proving the presence of the bond between the reinforcement and the concrete throughout the test. Fig.4.8.c shows the specimen after stripping the concrete cover.

The load vs. deflection curve of this specimen is shown in Fig.4.9. The load carrying capacity decreased by only 7% in the 5th cycle, along with a decrease in the stiffness. However, no pinching was observed in

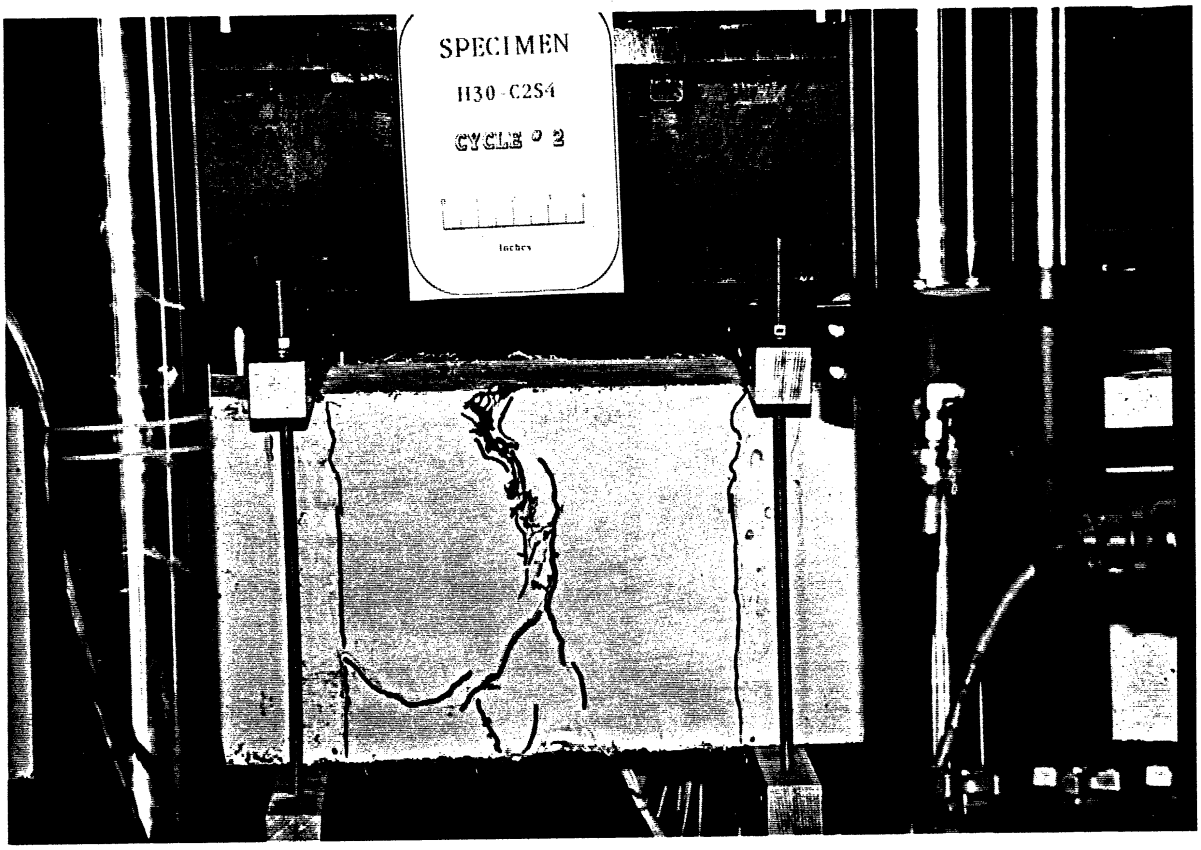

Fig. 4.8- a) Specimen at second cycle.

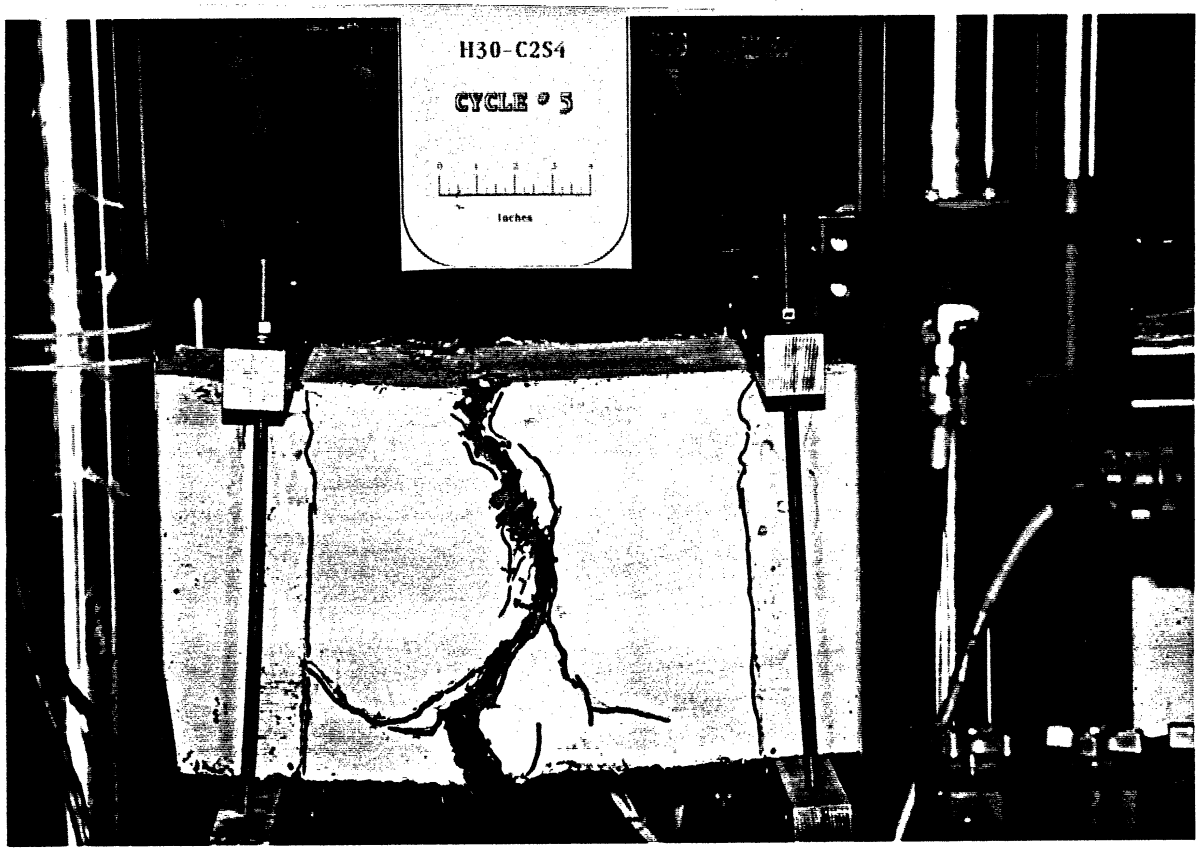

Fig. 4.8- b) Specimen at failure.

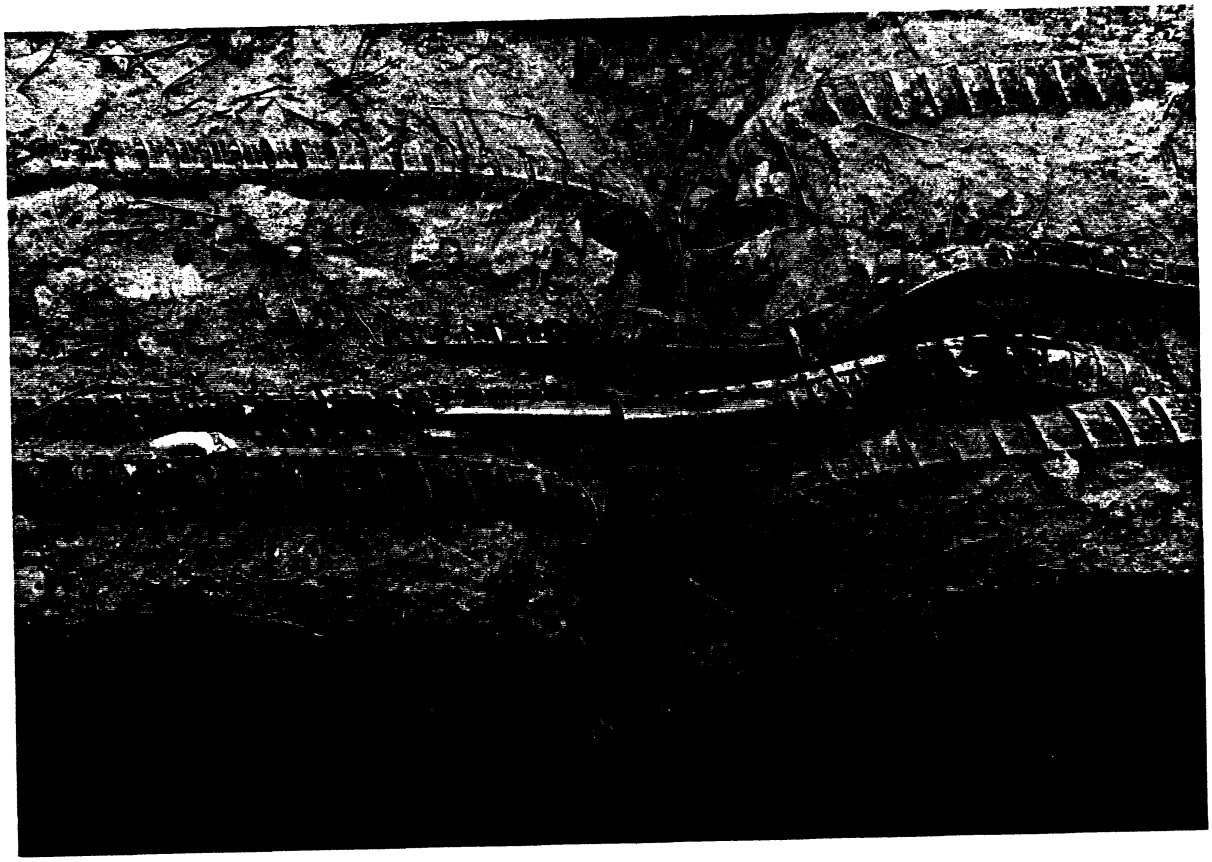

Fig. 4.8- c) Specimen after stripping the concrete cover.

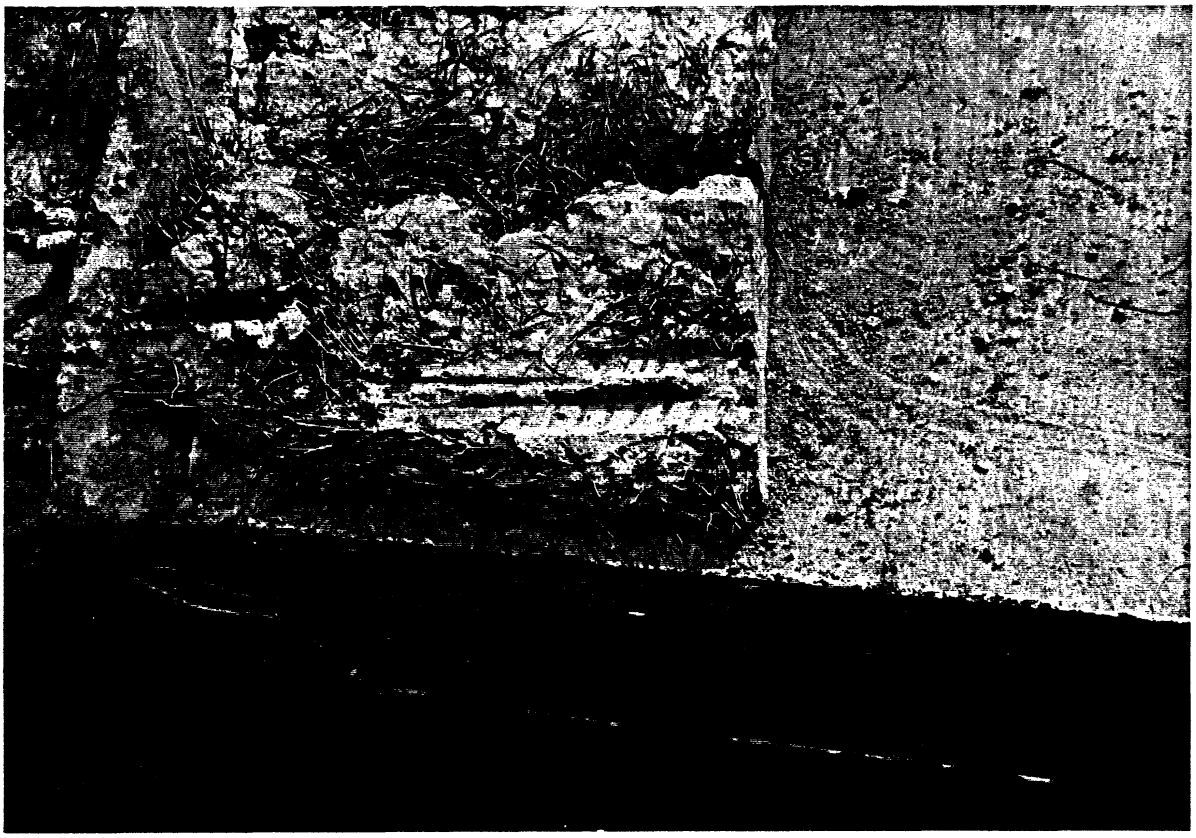

Fig. 4.8- d) Concrete cover.

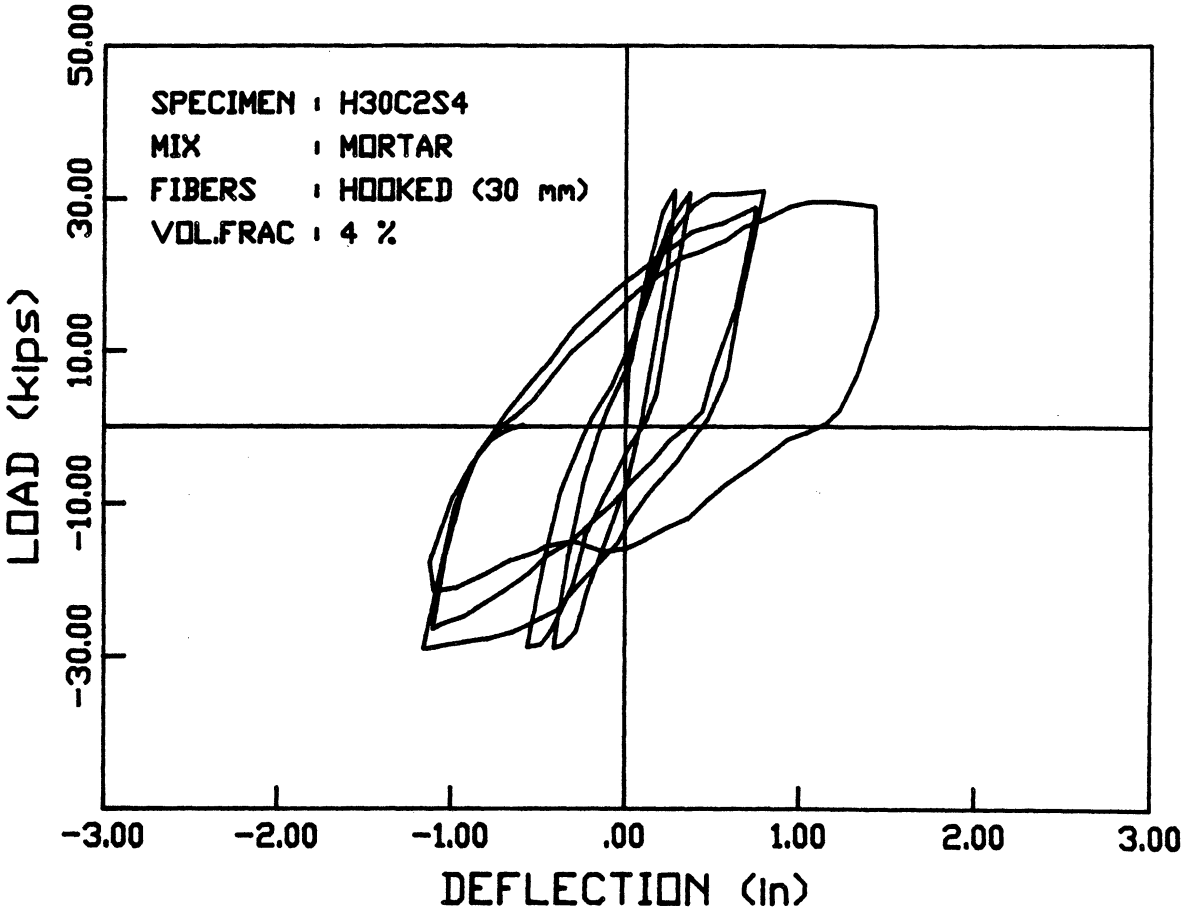

Fig. 4.9- Load vs. deflection curve.

the hysteresis loop for that load cycle. It can therefore be noted that the overall specimen behavior was adequate up to failure which was caused by the sudden rupture of the tension reinforcing bars.

Specimen D30C2S4:

A single flexural crack appeared in the middle of the CIP joint. Another flexural crack appeared at the interface, along with shear cracks in the precast beam parts. However, only the flexural crack inside the CIP joint continued to widen. During the 5th loading cycle the crack was 3/4 in. wide. The resulting stress concentrations in the reinforcing steel led to failure of all 4 reinforcing bars, and consequently, failure of the specimen. The maximum displacement ductility was 3.5. Fig.4.10 shows the specimen in the second loading cycle and at failure. No slippage of the reinforcing bars occurred, as was verified later. Fig.4.10.c shows the specimen after stripping the concrete cover.

The load vs. deflection curve of this specimen is shown in Fig.4.11. The load carrying capacity decreased by only 3% in the 5th cycle, along with a decrease in the stiffness. No pinching was observed in the hysteresis loop since only 4 full loading cycles were completed.

Specimen H30CON2.1:

During the first two loading cycles several flexural cracks appeared inside the CIP joint. Flexural cracks also appeared at the interface, as well as shear cracks in the precast beam parts. As observed earlier, only one flexural crack inside the CIP joint continued to widen. Failure occurred at the start of the 5th loading cycle, inside the CIP joint, in the

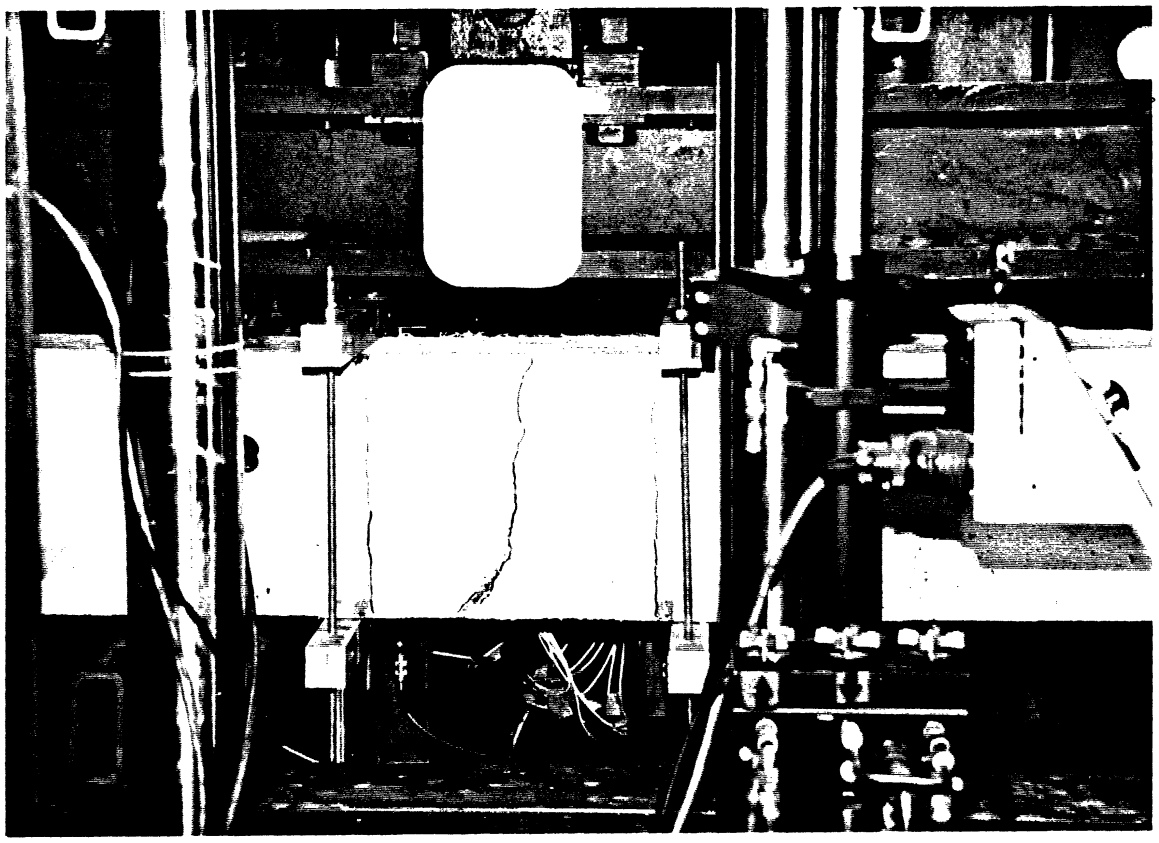

Fig. 4.10- a) Specimen at second cycle.

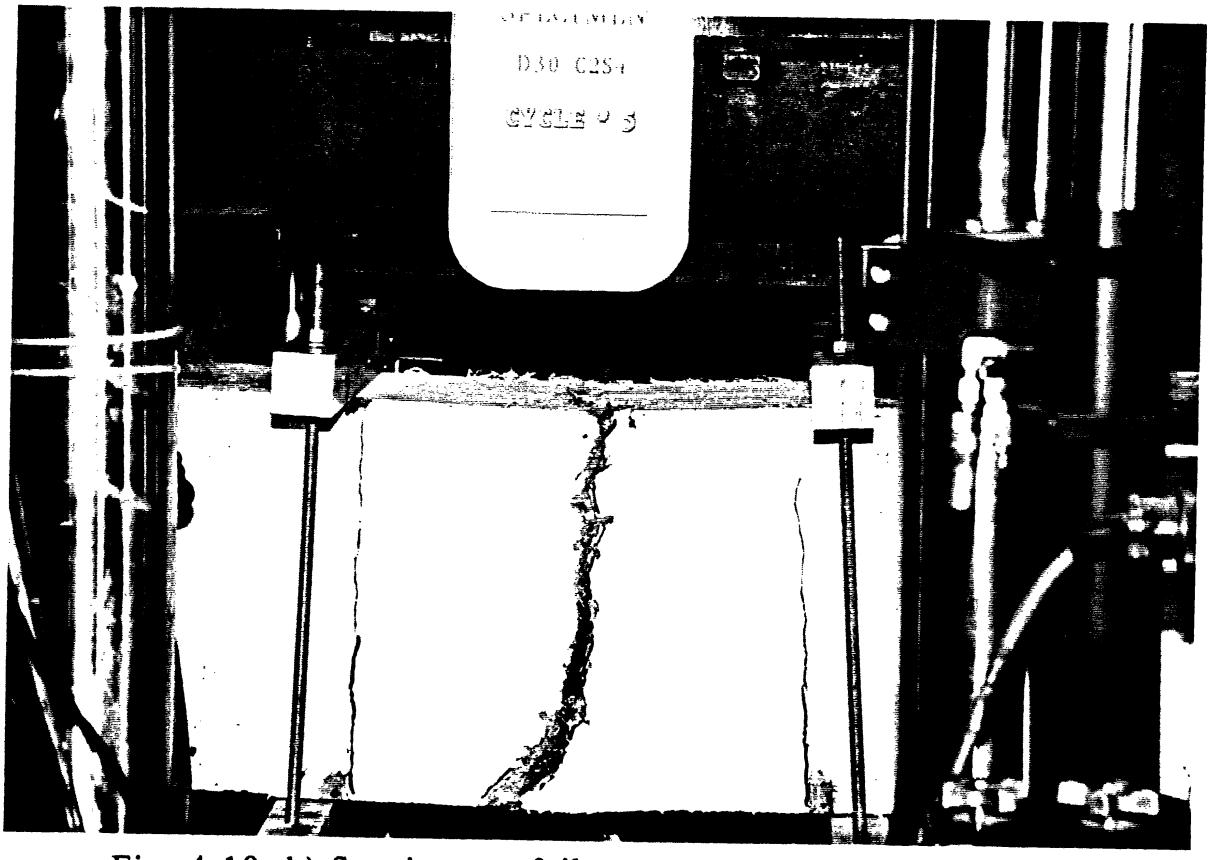

Fig. 4.10- b) Specimen at failure.

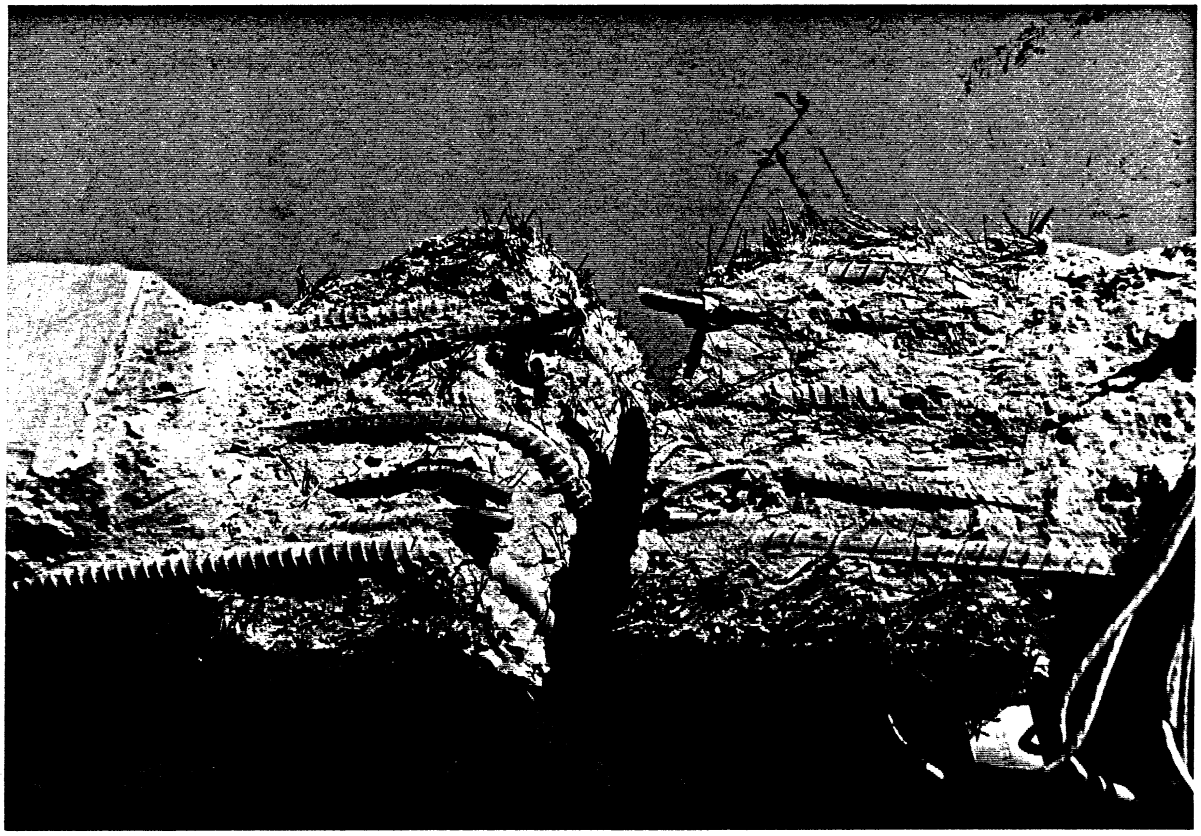

Fig. 4.10- c) Specimen after stripping the concrete cover.

Fig. 4.10- d) Concrete cover.

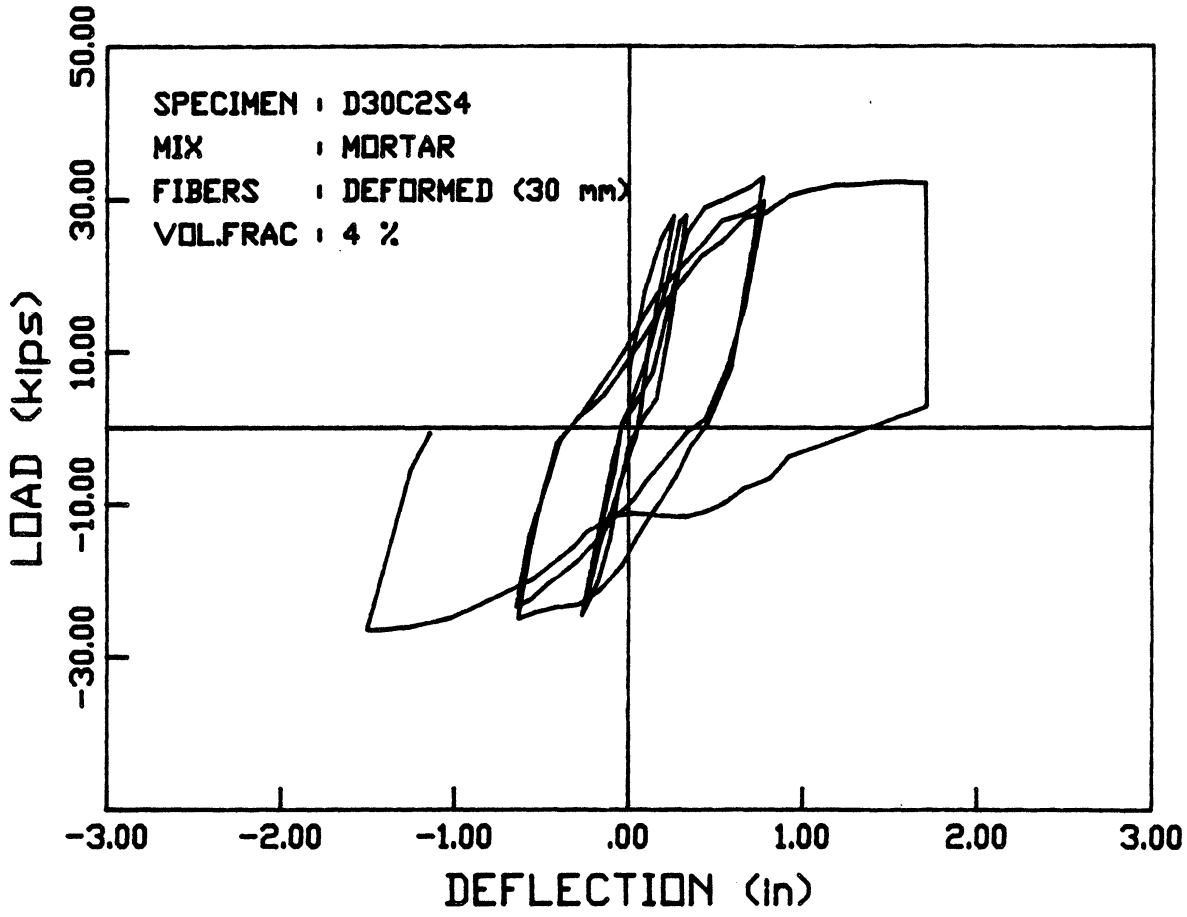

Fig. 4.11- Load vs. deflection curve.

downward loading portion. The failure was caused by the tension rupture of one reinforcing bar inside the joint. The maximum displacement ductility was 4.0. Fig.4.12 shows the specimen in the second loading cycle and at failure. No slippage of the reinforcing bars occurred.

The load vs. deflection curve of this specimen is shown in Fig.4.13. The load carrying capacity did not decrease in the 5th cycle, despite the decrease in the stiffness. Here also, no pinching was observed in the hysteresis loop.

Specimen D30CON2.1:

Again, the same cracking pattern was observed; several flexural cracks inside the joint and at the interface, and shear cracks in the precast beam parts. A single flexural crack inside the joint developed into a major crack and continued to widen, while the other cracks remained the same. Failure occurred at the start of the 6th loading cycle, inside the CIP joint, in the downward loading portion. This failure was caused by the tension rupture of one reinforcing bar inside the joint. The maximum displacement ductility was 4.0. Fig. 4.14 shows the specimen in the second loading cycle and at failure. No slippage of the reinforcing bars occurred.

The load vs. displacement curve for this specimen is shown in Fig. 4.15. The load carrying capacity did not decrease in the 5th cycle, despite the decrease in the stiffness. No pinching was observed in the hysteresis loop.

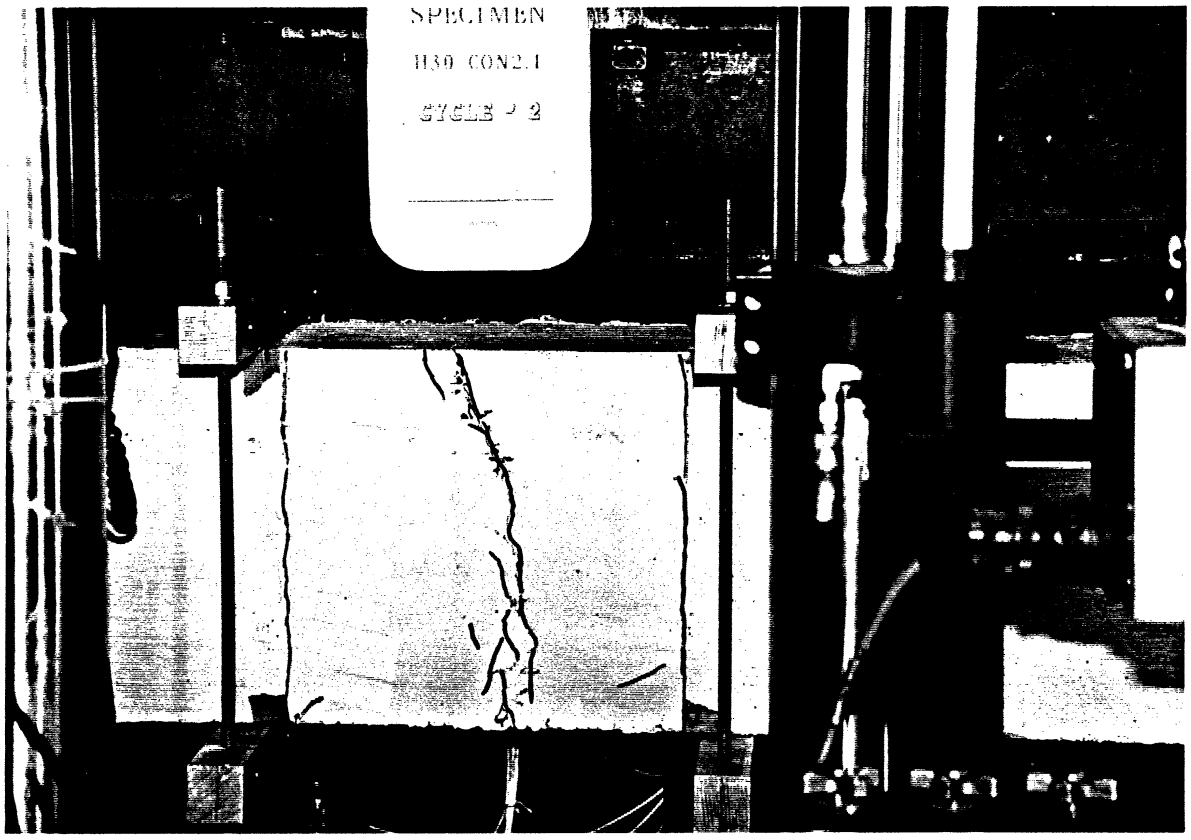

Fig. 4.12- a) Specimen at second cycle.

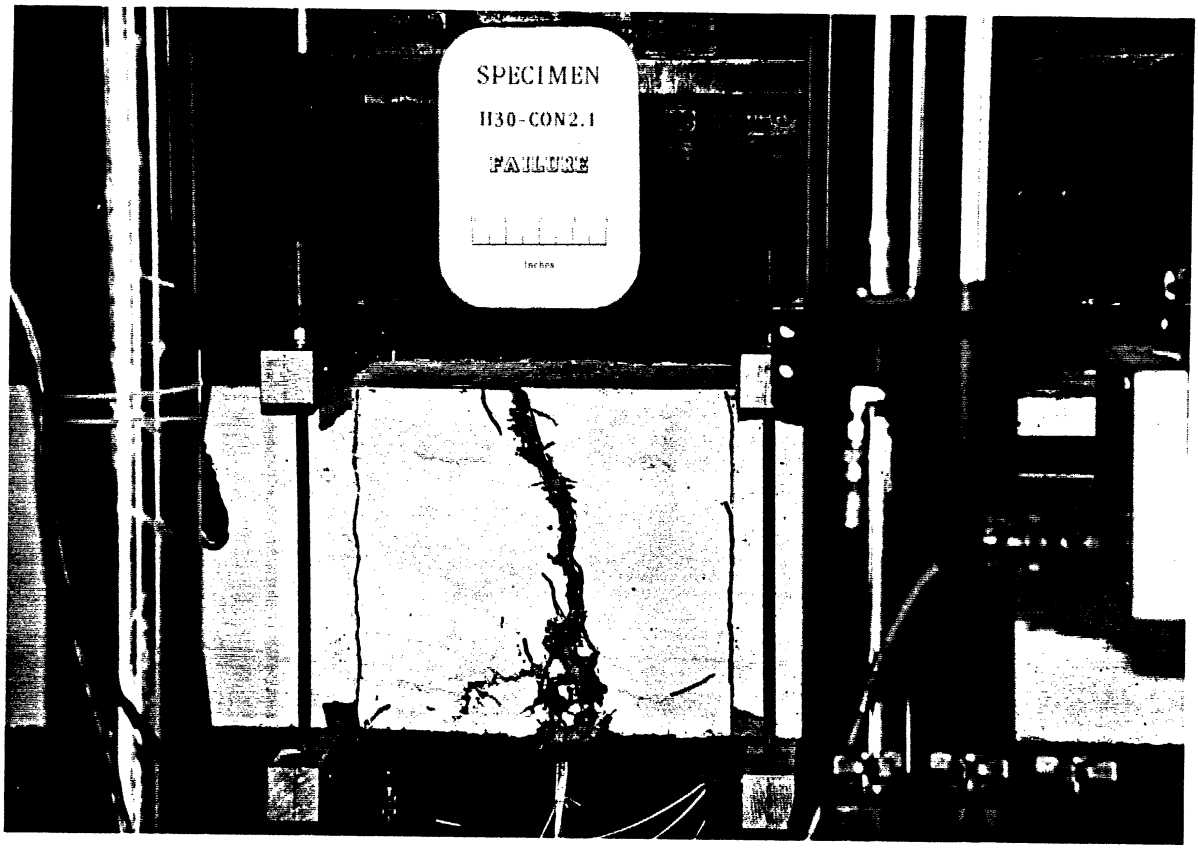

Fig. 4.12- b) Specimen at failure.

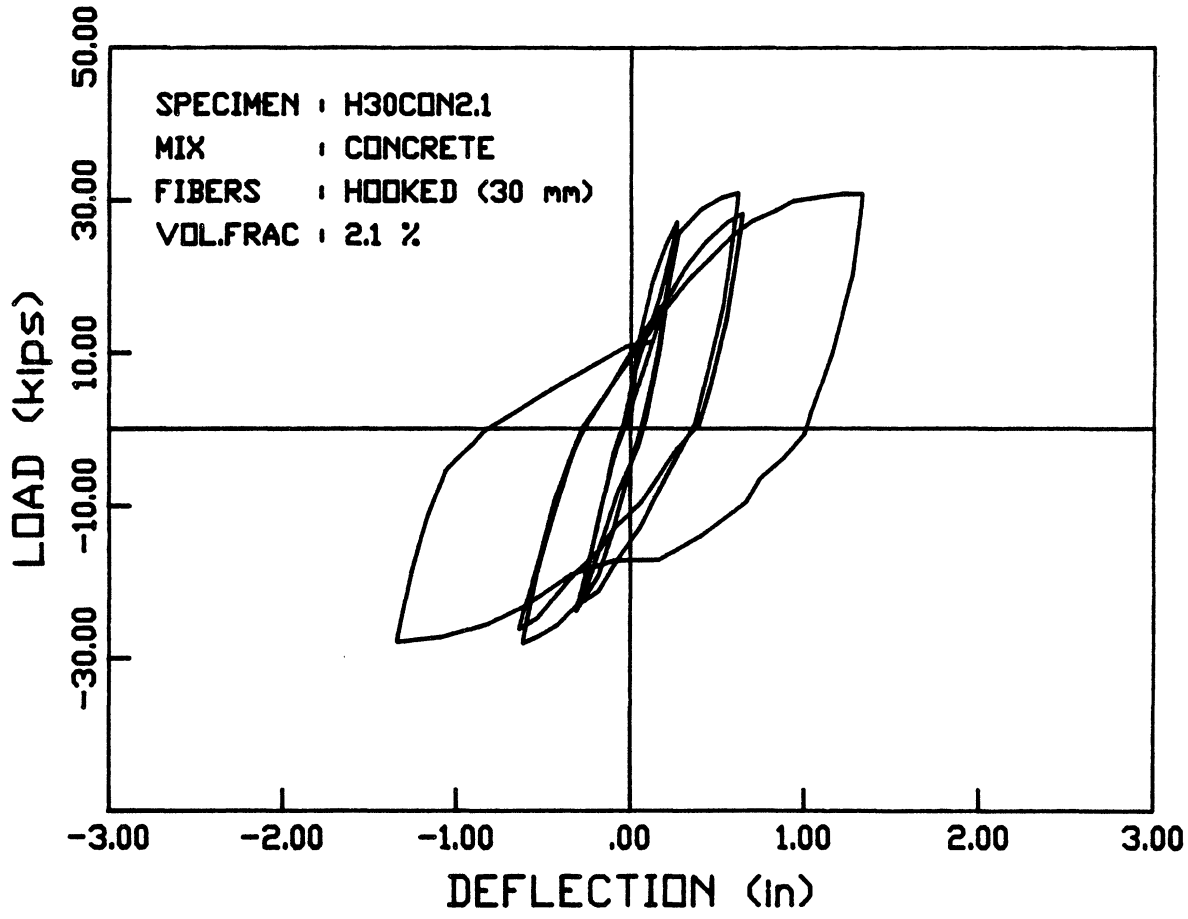

Fig. 4.13- Load vs. deflection curve.

Fig. 4.14- a) Specimen at second cycle.

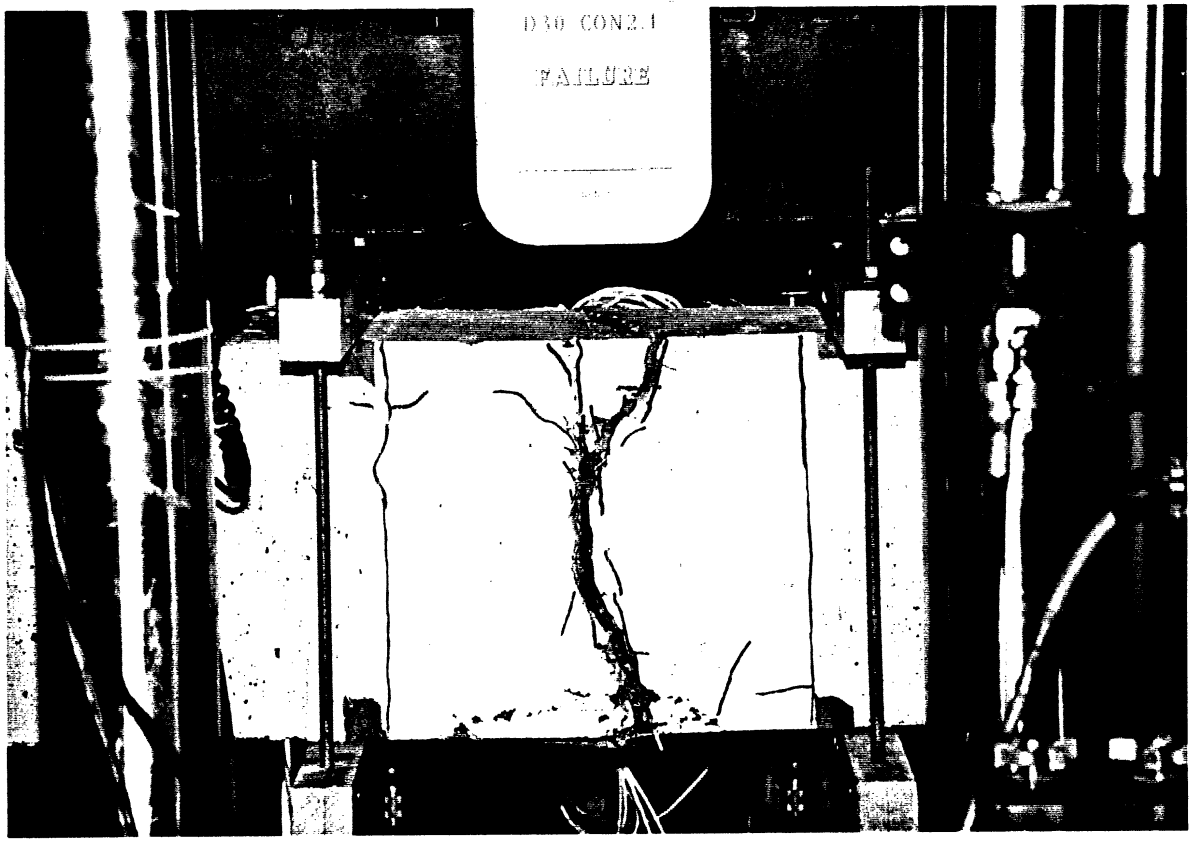

Fig. 4.14- b) Specimen at failure.

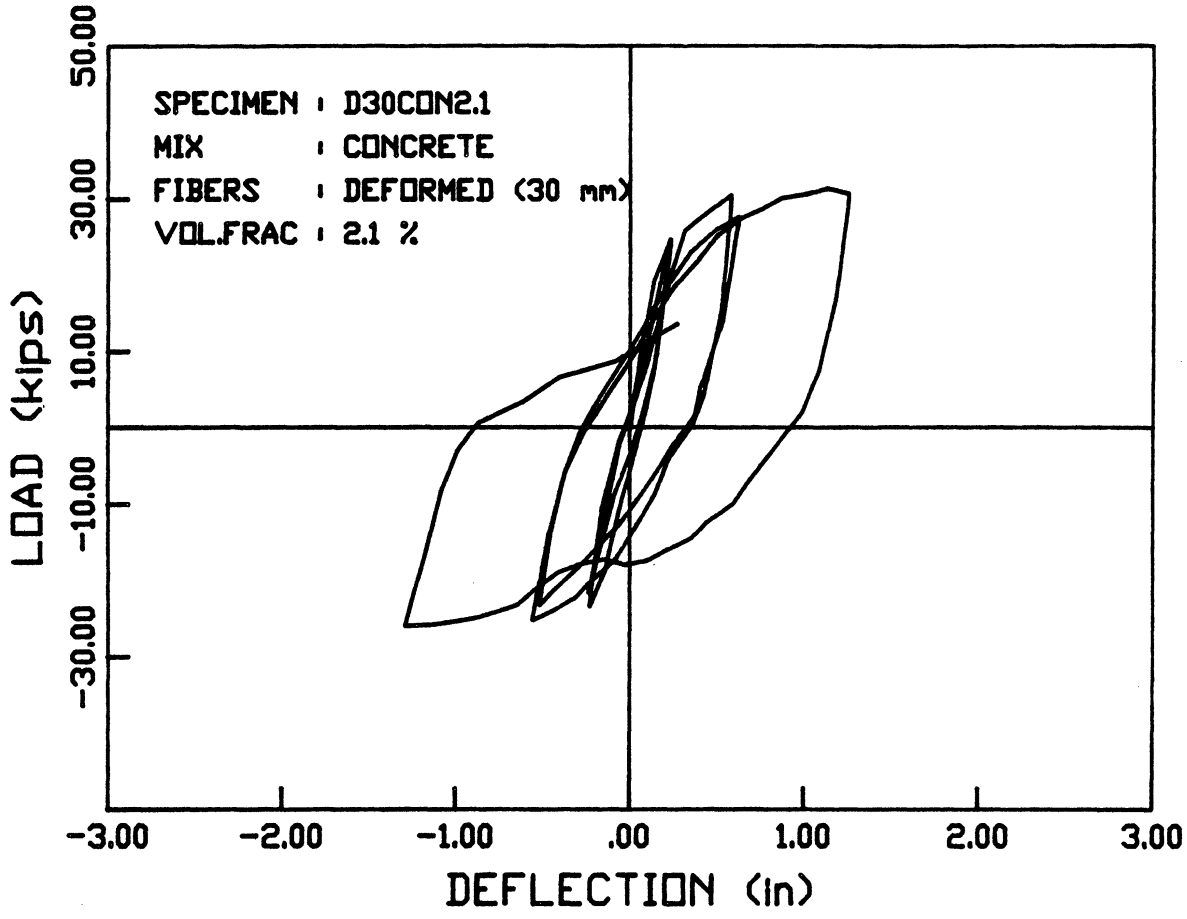

Fig. 4.15- Load vs. deflection curve.

Specimen H50CON1:

Several flexural cracks appeared in the middle of the CIP joint and at the interface. Shear cracks also appeared in the precast beam parts. However, as observed in all previous specimens, only one flexural crack inside the CIP joint continued to widen. Failure occurred in the 5th loading cycle, inside the CIP joint, in the upward loading portion. This failure was caused by the consecutive tension rupture of two reinforcing bars inside the joint. The maximum displacement ductility was 3.8. Fig. 4.16 shows the specimen in the second loading cycle and at failure. No slippage of the reinforcing bars occurred.

The load vs. displacement curve for this specimen is shown in Fig. 4.17. The load carrying capacity decreased by only 4% in the 5th cycle, accompanied by a decrease in the stiffness. No pinching was observed in the hysteresis loops.

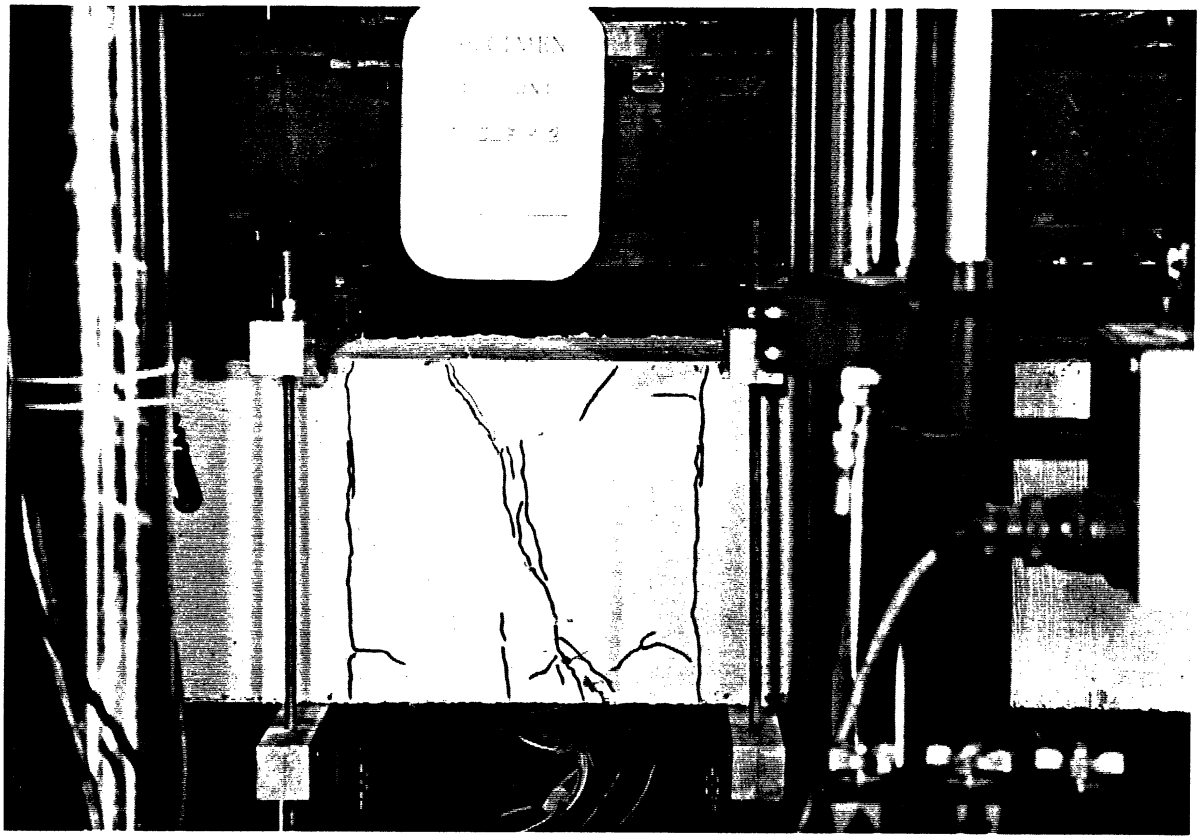

Fig. 4.16- a) Specimen at second cycle.

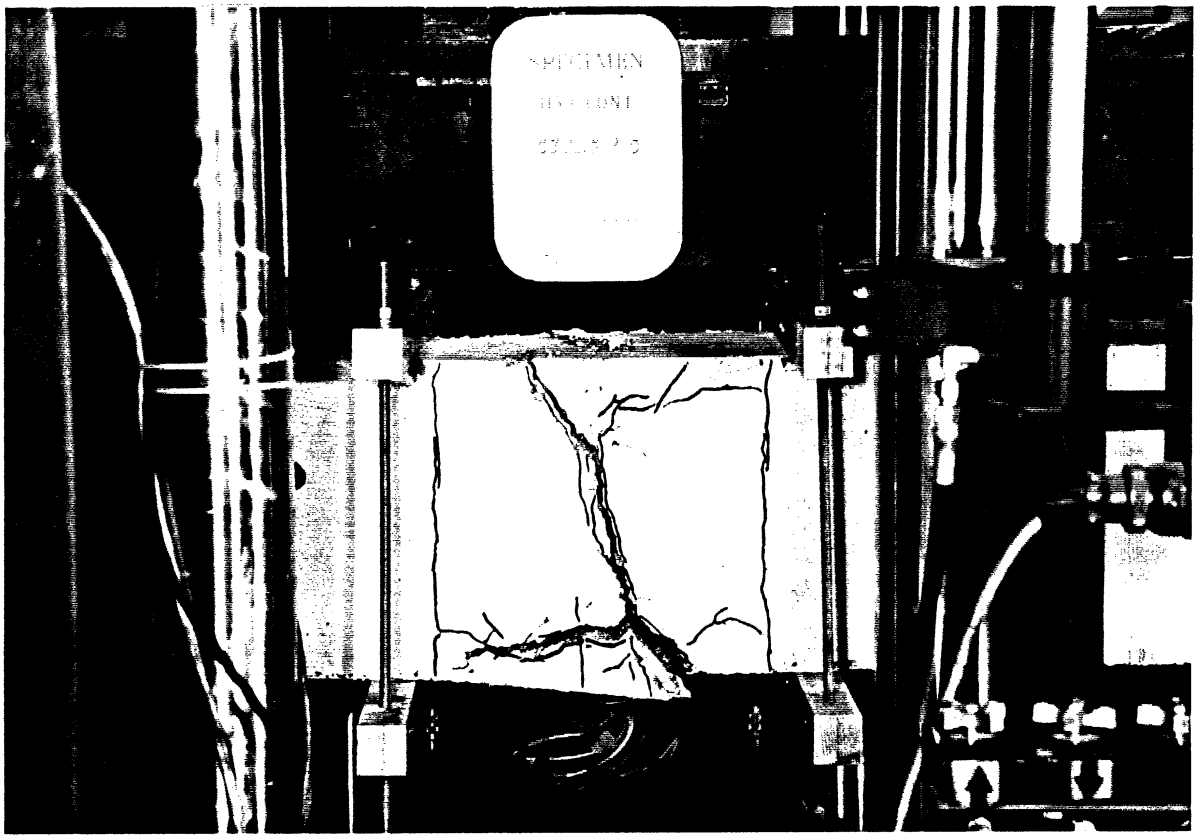

Fig. 4.16- b) Specimen at failure.

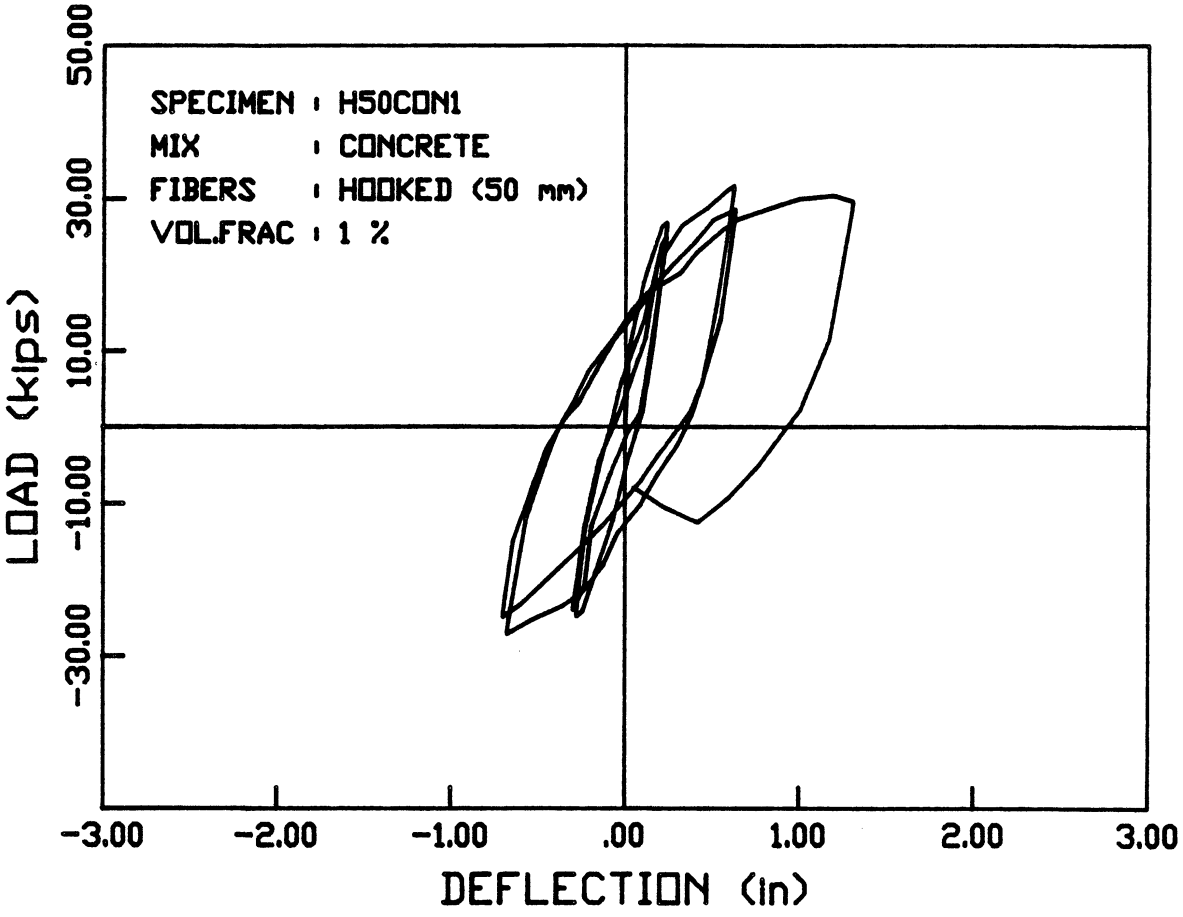

Fig. 4.17- Load vs. deflection curve.

CHAPTER V

DISCUSSION OF TEST RESULTS

5.1 -General

In this chapter, the test results of the beam specimens are discussed using the data from the load vs. displacement curves. A comparison is made among the specimens to determine the effectiveness of the different composites used in the beams cast-in-place (CIP) joints. The specimens are also compared to a "control" specimen in which plain concrete is used as the matrix in the CIP joint.

The control specimen was tested by Abdou (2) in a previous investigation where slurry infiltrated concrete (SIFCON) was used as the composite in the CIP joint. The specimen had the same reinforcing arrangement of the specimens tested in this investigation. The loading history of the control specimen is shown in Fig. 5.1. The behavior of the specimen was characterized by a localized plastic hinge in the CIP joint. Failure occured due to the crushing of concrete after reaching the specimen's maximum load carrying capacity. The load vs. deflection curve of the control specimen is shown in Fig. 5.2. Although the loading

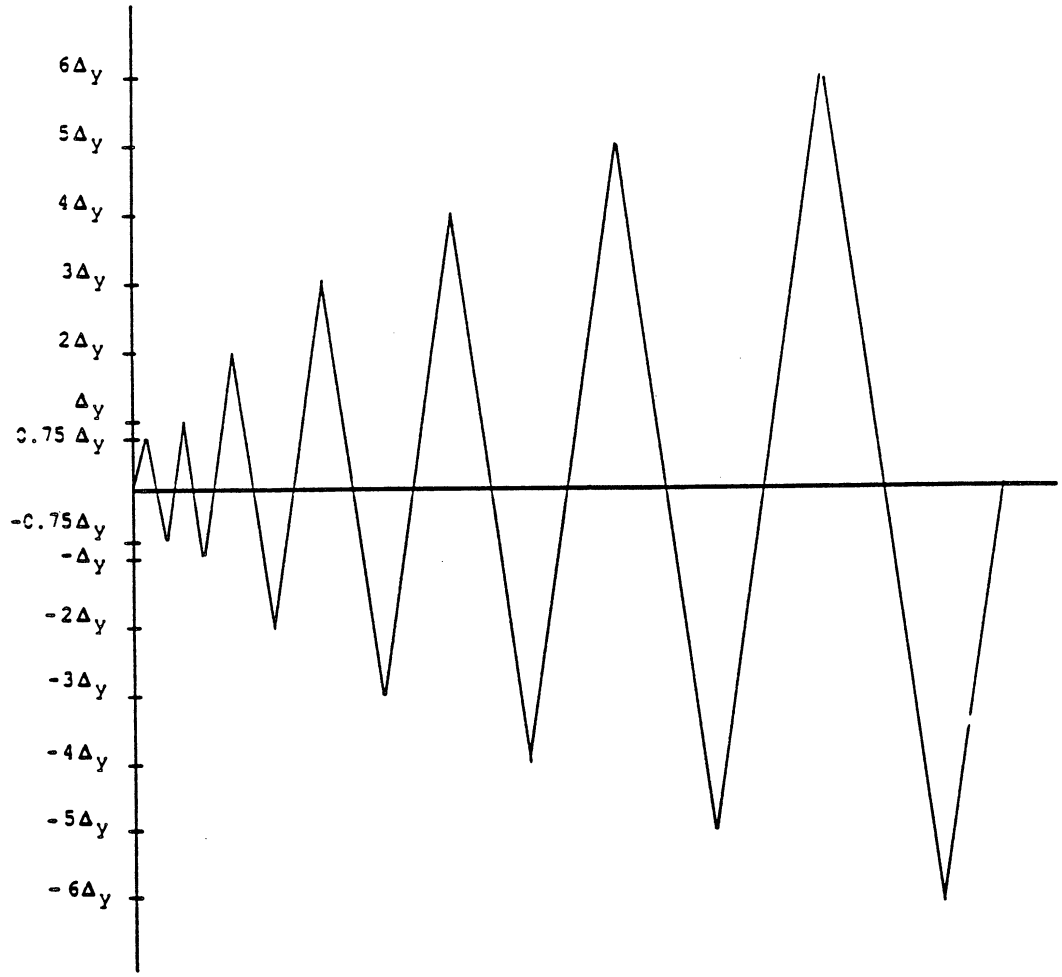

Fig. 5.1- Loading history of control specimen. (2)

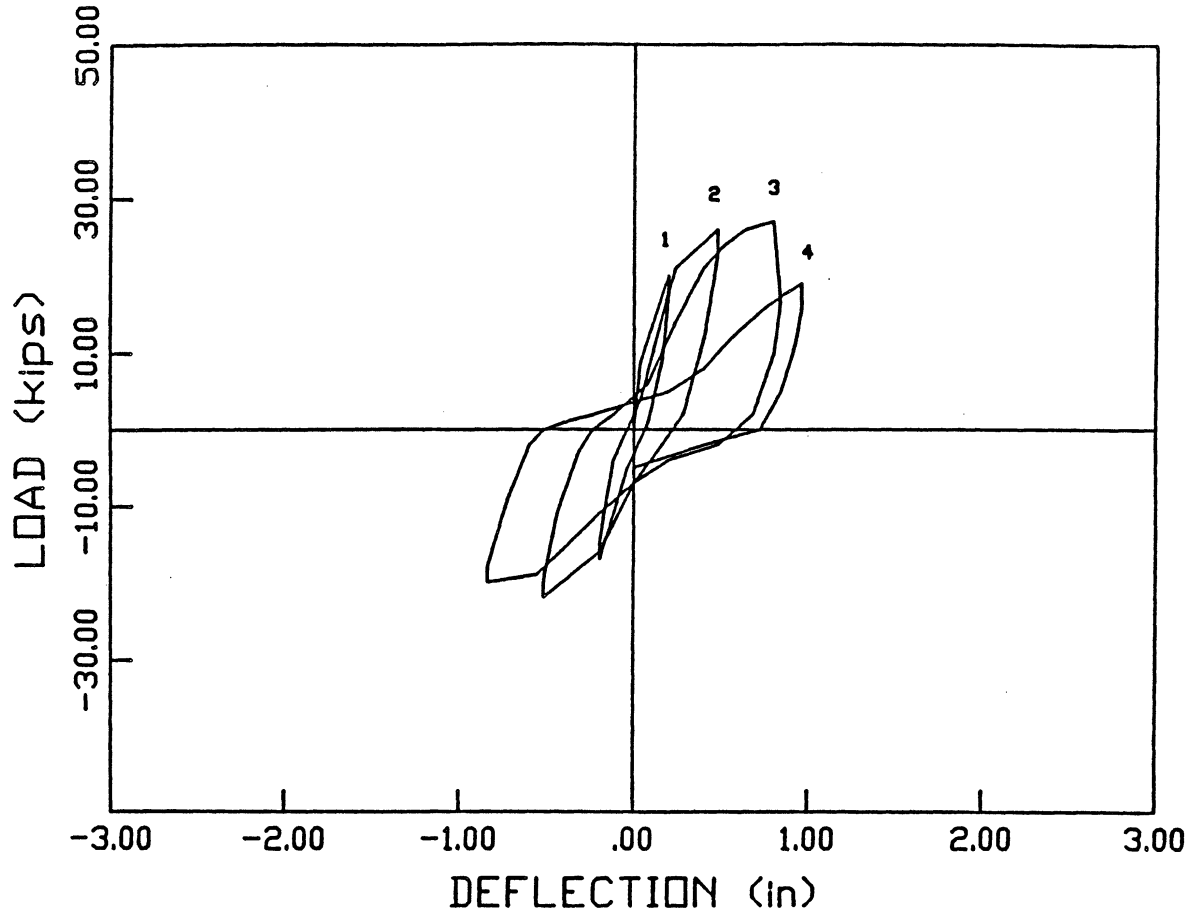

Fig. 5.2- Load vs. deflection curve of control specimen. (2)

history for the control specimen is not identical to that used for the specimens in this investigation, reasonable comparisons and conclusions can be made.

In discussing and comparing the test results, three parameters are used: 1) diplacement ductility, 2) load carrying capacity, and 3) energy dissipation.

5.2 -Displacement Ductility

The maximum displacement of each cycle related to the yield cycle is refered to as the displacement ductility. The displacement ductilities for all the specimens are given in Table 5.1.

The maximum displacement ductility for the control specimen was 2.5. Higher displacement ductilities were observed for the specimens with fiber reinforced concrete (FRC) cast-in-place (CIP) joints. For specimen POLYCS4, the maximum displacement ductility observed was 5.8. For the other specimens, diplacement ductilities around 4.0 were observed.

5.3 -Load Carrying Capacity

The maximum load applied to each specimen at each cycle was compared to the maximum load applied to that specimen in the first yield cycle. The resulting ratio was used to trace the load carrying capacity throughout the test, as well as to compare the changes in this capacity for different specimens. The values for this ratio at different cycles, for all the specimens, is given in Table 5.2.

Table 5.1- Displacement ductilities.

Ratio of the Maximum Displacement at each Cycle to that of the First Yield Cycle								
Specimen	**Cycle Number**							
	1	2	3	4	5	6	7	8
CONTROL	0.5	1.0	2.0	2.5	---	---	---	---
POLYCS4	1.0	1.0	2.0	2.0	4.0	4.0	5.8	5.8
H30C2S4	1.0	1.0	2.0	2.0	3.3	---	---	---
D30C2S4	1.0	1.0	2.0	2.0	3.5	---	---	---
H30CON2.1	1.0	1.0	2.0	2.0	4.0	---	---	---
D30CON2.1	1.0	1.0	2.0	2.0	4.0	---	---	---
H50CON1	1.0	1.0	2.0	2.0	3.8	---	---	---

Table 5.2- Load carrying capacities.

Ratio of the Maximum Load at Each Cycle to that of the First Yield Cycle								
Specimen	**Cycle Number**							
	1	2	3	4	5	6	7	8
CONTROL	0.77	1.00	1.04	0.73	---	---	---	---
POLYCS4	1.00	0.96	1.28	1.21	1.37	1.03	1.15	0.63
H30C2S4	1.00	1.00	1.00	0.93	0.93	---	---	---
D30C2S4	1.00	1.00	1.18	1.07	1.15	---	---	---
H30CON2.1	1.00	0.95	1.14	1.04	1.13	---	---	---
D30CON2.1	1.00	1.00	1.24	1.12	1.27	---	---	---
H50CON1	1.00	0.93	1.18	1.07	1.13	---	---	---

A 4% increase beyond the yield load was observed for the control specimen. The specimen failed in the 4th cycle, at a displacement ductility of 2.5, after losing 27% of its load carrying capacity. A much improved behavior was observed for all the other specimens. Increases in the load carrying capacity of 14%, 18%, 27%, and 37% beyond the yield load were observed for the tested specimens. Specimen POLYCS4 sustained 8 cycles before failure at a diplacement ductility of 5.8 with its load carrying capacity decreasing by 37%. Specimen H30C2S4 sustained 5 cycles before failure at a diplacement ductility of 3.3 with its load carrying capacity decreasing by only 7%. The rest of the specimens sustained 5 cycles before failure at a diplacement ductility of about 4.0 with increasing load carrying capacity.

Comparing the individual specimens, specimen POLYCS4, which survived the 5th loading cycle, did not experience a loss in its load carrying capacity until the 6th loading cycle. The other specimens, which did not survive the 5th loading cycle, also did not experience a significant loss in their load carrying capacity until the 5th cycle, when they failed. However, the load level before failure was higher for these specimens. The fact that specimen POLYCS4 sustained 8 cycles and exhibited significant loss in its load carrying capacity could be related to the low strength of the CIP joint composite used compared to other specimens.

5.4 -Energy Dissipation

For all specimens the energy dissipated in each cycle was calculated then normalized with respect to the energy dissipated during the first yield

Table 5.3- Energy dissipation of the specimens.

Ratio of the Energy Dissipation of Each Cycle to that of the First Yield Cycle								
Specimen	**Cycle Number**							
	1	2	3	4	5	6	7	8
CONTROL	0.2	1.0	2.05	---	---	---	---	---
POLYCS4	1.0	0.7	3.6	2.9	11.4	8.5	12.6	---
H30C2S4	1.0	1.3	5.8	4.5	7.5	---	---	---
D30C2S4	1.0	0.9	8.9	7.1	---	---	---	---
H30CON2.1	1.0	0.7	5.4	4.8	16.3	---	---	---
D30CON2.1	1.0	0.5	5.9	5.1	18.5	---	---	---
H50CON1	1.0	0.5	4.7	4.2	---	---	---	---

cycle. The normalized energy dissipation for all specimens is given in Table 5.3.

The control specimen survived three complete cycles only. The maximum energy dissipated was 2.05. The FRC specimens exhibited considerably larger energy dissipation and survived at least four complete cycles. Energy dissipation values of 4.7, 7.5, 8.9, 12.6, 16.3, and 18.5 were observed. Comparing the individual specimens, The concrete composites containing hooked and deformed short steel fibers exhibited the highest energy dissipation, along with the mortar composite containing plastic fibers.

CHAPTER VI

SUMMARY AND CONCLUSIONS

6.1 -Summary

The experimental program was aimed at developing a strong, ductile, and energy dissipating connector between precast elements. Fiber reinforced concrete (FRC) composites were used as the connector materials since they were found to provide adequate ductility and energy dissipation.

6.1.1 -Part I

The first part of the investigation involved the testing, under compression, of various FRC composites. The purpose of these compression tests was to identitfy the characteristics of the composites, such as strength and toughness, and then to select the composites suitable to be placed as a connector between precast elements. Therefore, thirty nine cylinders containing various FRC composites were tested under compression. The variables studied were:

- Matrix type: Three types of matrices were tested: 1) a mortar mix containing 1 part cement and 1 part sand; 2) a mortar mix containing 1 part cement and 2 parts sand; and 3) a concrete mix containing 1 part cement, 2.5 parts sand, and 2.1 parts aggregate.

- Fiber type: Six types of fibers were used: 1) polypropylene plastic fibers of 3/4 in. length; 2) crimped steel fibers of 1 in. length; 3) flat steel fibers of 3/4 in. length; 4) hooked steel fibers of 30 mm length; 5) deformed steel fibers of 30 mm length; and 6) hooked steel fibers of 50 mm length.

- Fiber volume fraction: Three fiber volume fractions were used: 1) V_f = 4% for all mortar mixes; 2) V_f = 2.1% for concrete mixes containing 30 mm hooked and deformed steel fibers; and 3) V_f = 1% for concrete mixes containing 50 mm hooked steel fibers.

The composites parameters are given in Table 3.1.

Based on the test results, it was decided that the composites containing hooked and deformed steel fibers, in both the mortar and the concrete matrices, should be used as material for the connector between the precast elements. Also selected were the the composite containing long hooked steel fibers in a concrete matrix, as well as the composite containing plastic polypropylene fibers in a mortar matrix. Table 4.6 shows the characteristics of the composites used in the beam specimens.

6.1.2 -Part II

In the second part of the investigation, six beam-type specimens were constructed and tested. Each specimen consisted of two precast concrete elements connected together to form a beam with a cast-in-place joint, fiber reinforced concrete being the cementitious material in the joint. The specimens were subjected to reversed cyclic third point loading which followed a specified loading history. For all specimens, the failure occurred inside the CIP joint. Failure was due to the opening of a single major flexural crack inside the CIP joint which caused stress concentrations in the renforcing bars. This led to the fracture of at least one of the bars in tension and consequently, failure of the specimens.

The maximum displacement ductility observed for the control specimen was 2.5. Larger displacement ductilities were achieved for all the specimens.

A 4% increase in the load carrying capacity beyond the yield load was observed for the control specimen. This was followed by a decrease of 27% of that capacity at failure. Significantly larger increases in the load carrying capacities were observed for all the FRC specimens (14%, 18%, 27%, and 37%). Except for specimen POLYCS4, which experienced a loss of 37% in its load carrying capacity in the 8th cycle, the specimens did not undergo a significant loss in their load carrying capacity until the 5th cycle, when they failed. Furthermore, the load level before failure was higher for these specimens.

A maximum energy dissipation of only 2.05 was observed for the control specimen. For all the specimens, however, significant increases in the energy dissipation were observed. Maximum energy dissipation values of 12.6, 16.3, and 18.5 were recorded.

6.2 -Conclusions

Based on the test results of the six beam-type specimens investigated, the following conclusions can be drawn:

1- Compared to the control specimen, a much improved behavior was observed for all the FRC specimens. Larger displacement ductilities were achieved, higher load levels were observed, and better energy dissipation values were recorded.

2- Comparing the individual specimens, it was noted that the specimens having a CIP joint containing steel fiber composites, despite not surviving the 5th loading cycle, exhibited better energy dissipation, higher stiffness, and higher load levels than the specimen with plastic fibers in the CIP joint.

3- The arrangement of the reinforcing steel was adequate in transferring the forces to the joint area. The success of the steel arrangement can be attributed to the fact that no slippage of the reinforcing bars occurred throughout the tests.

4- The presence of a single crack in the CIP joint led to localized failure of the specimens. This failure was represented by the fracture of at least one reinforcing bar. For the specimen that

survived the 5th loading cycle, the failure was preceded by stiffness degradation and pinching in the hysteresis loop.

6.2.1 -Present Research

1. The presence of a single flexural crack in the CIP joint proved to be detrimental to the behavior of the specimens. It is believed that a distribution of the flexural cracks inside the CIP joint would improve the behavior of the joint. Therefore, the following solutions are proposed to achieve that purpose:

a) A modified arrangement of the reinforcing bars in the CIP joint. This arrangement would, simultaneously, ensure multiple cracking in the joint, and, as in the present steel arrangement, provide the necessary bond to transfer the forces across the joint.

b) An adequate ratio of moment capacities between sections inside the CIP joint and at the interfaces.

c) A larger plastic hinging zone. The sudden decrease in the reinforcement inside the joint over a small length was one of the causes of the development of a single crack and, hence, the localized failure of the specimen. Therefore, a larger hinging zone is proposed to allow for the distribution of the cracks in the joint and, thereby, improve the overall specimen behavior.

2. The beam specimens tested in this investigation were subjected to cyclic third point loading. This loading subjected the middle third of the beam, which included the CIP joint, to a constant moment and no shear. However, since a moment gradient and shear forces are present when

beam-to-column connections are loaded, the testing of more realistic connections is necessary to evaluate the effectivness of the FRC composites in providing the desired properties under cyclic loading.

REFERENCES

1. Abdel-Fattah, B. A., and Wight, J. K., "Experimental Study of Moving Plastic Hinging Zones for Earthquake Resistant Design of Reinforced Concrete Buildings", Report No. UMCE 85-11, Department of civil Engineering, The University of Michigan, Ann Arbor, December 1985.

2. Abdou, H. M., Naaman, A. E., and Wight, J. K., "Cyclic Response of Reinforced Concrete Connections Using Cast-in-place SIFCON Matrix", Report No.UMCE 88-8, Department of Civil Engineering, The University of Michigan, Ann Arbor, August 1988.

3. "Building Code Requirements for Reinforced Concrete", (ACI 318-83), Committee 318, American Concrete Institute, Detroit, Michigan, 1983.

4. ACI Committee 544, "State-of-the-Art Report on Fiber Reinforced Concrete", American Concrete Institute, Detroit, 1984.

5. Al Haddad, M. S., and Wight, J. K., "Feasibility and Consequences of Moving Beam Plastic Hinging Zones for Earthquake Resistant Design of R/C Buildings", Report No. UMCE 86-1, Department of civil Engineering, The University of Michigan, Ann Arbor, July 1986.

6. ATC-8 Seminar, "Design of Prefabricated Concrete Buildings for Earthquake Loads", Proceedings, ATC, Berkely, California, January 1982.

7. Code of Practice for the Design of Concrete Structures", NZS 3101: 1982, Standard Association of New Zealand, Wellington, New Zealand.

8. Craig, R. J., Mahadev, S., Patel, C. C., Viteri, M., and Ketesz, C., "Behavior of Joints Using Reinforced Fibrous Concrete", Symposium on Fiber Reinforced Concrete, ACI Special Publication, SP-81, ACI, Detroit, 1984.

9. Craig, R. J., Mc Connell, J., Germann, H., Dib, N., and Kashani, F., "Behavior of Reinforced Concrete Fibrous Columns", Symposium on Fiber Reinforced Concrete, ACI Special Publication, SP-81, ACI, Detroit, 1984.

10. Dolan, C., Stanton, J., and Anderson, R., "Moment Resistant Connections and Simple Connections", PCI Journal, Vol. 32, March-April 1987.

11. Durani, A. J., and Wight, J. K., "Experimental and Analytical Studies of Interior Reinforced Concrete Beam-to-Column Connections", Report No. UMEE 82R3, Department of civil Engineering, The University of Michigan, Ann Arbor, July 1982.

12. Englekirk, R., "Concepts for the Development of Earthquake Resistant Ductile Frames of Precast Concrete", PCI Journal, Vol. 32, January-February 1987.

13. Englekirk, R., "Overview of ATC Seminar of Prefabricated Concrete Buildings for Earthquake Loads", PCI Journal, Vol. 27, January-February 1982.

14. Hawkins, N., and Englekirk, R., "U. S. - Japan Seminar on Precast Concrete Construction in Seismic Zones", PCI Journal, Vol. 32, March-April 1987.

15. Henager, C. H., "Steel Fibrous Ductile Concrete Joint for Seismic Resistant Structures", ACI Publication SP-53, Symposium on Reinforced Concrete Structures in Seismic Zones, 1974 ACI Annual Convention.

16. Jindal, R. L., "Shear and Moment Capacities of Steel Fiber Reinforced Concrete Beams", Symposium on Fiber Reinforced Concrete, ACI Special Publication, SP-81, ACI, Detroit, 1984.

17. Jindal, R. L., and Hassan, K. A., "Behavior of Steel Fiber Reinforced Concrete Beam-Column Connections", Symposium on Fiber Reinforced Concrete, ACI Special Publication, SP-81, ACI, Detroit, 1984.

18. Jindal, R., and Sharma, V., "Behavior of Steel Fiber Reinforced Concrete Knee-Type Beam-Column Connections", Fiber Reinforced Concrete - Properties and Applications, SP-105, ACI, Detroit, 1987.

19. Lee, D. L., Wight, J. K., and Hanson, R. D., "Original and Repaired Reinforced Concrete Beam-Column Subassemblages Subjected to Earthquake Type Loading", Report No. UMEE 76S4, Department of civil Engineering, The University of Michigan, Ann Arbor, 1976.

20. Naaman, A. E., Wight, J. K., and Abdou, H. M., "SIFCON Connections for Seismic Resistant Frames", Concrete International Journal, Vol. 9, No. 11, ACI, November 1987.

21. Paulay, T., and Park, R., "Joints in Reinforced Concrete Frames Designed for Earthquake Resistance", Report No. 84-9, Department of Civil Engineering, University of Canterbury, Cristchurch, New Zealand, June 1987.

22. "Recommendations for Design of Beam-to-Column Joints in Monolithic Reinforced Concrete Structures", ACI-ASCE Joint Committee 352, Journal of American Concrete Institute, Proceedings, V. 82, No. 3, May-June 1985.

23. Scribner, C. F., and Wight, J. K., "Delaying Shear Strength Decay in Reinforced Concrete Members Under Large Load Reversals", Report No. UMEE 78R2, Department of civil Engineering, The University of Michigan, Ann Arbor, May 1978.

24. Sood, V., and Gupta, S., "Behavior of Steel Fibrous Concrete Beam-Column Connections", Fiber Reinforced Concrete - Properties and Applications, SP-105, ACI, Detroit, 1987.

UNCITED REFERENCES

1. ACI Committee 544, "Measurment of Properties of Fiber Reinforced Concrete", American Concrete Institute, Detroit, 1984.

2. Batson, G., Jenkins, E., and Spatney, R., "Steel Fibers as Shear Reinforcement in Beams", ACI Journal, Vol. 69, October 1972.

3. Bertero, V. V., and Popov, E. P., "Seismic Behavior of Ductile Moment Resisting Reinforced Concrete Frames", ACI Publication SP-53, Symposium on Reinforced Concrete Structures in Seismic Zones, 1974 ACI Annual Convention.

4. Castro, J., and Naaman, A. E., "Cement Mortar Reinforced with Natural Fibers", ACI Journal, Proceedings, Vol. 78, No. 1, January-February 1981.

5. Craig, R. J., "Structural Applications of Reinforced Fibrous Concrete", Concrete International Journal, Vol. 6, No. 12, ACI, December 1984.

6. Fanella, D. A., and Naaman, A. E., "Stress-Strain Properties of Fiber Reinforced Mortar in Compression", ACI Journal, Proceedings, Vol. 82, No. 4, July-August 1985.

7. Homrich, J. R., and Naaman, A. E., "Stress-Strain Properties of SIFCON in Uniaxial Compression and Tension", Report No. UMCE 87-7, Department of Civil Engineering, The University of Michigan, Ann Arbor, October 1987.

8. Johnston, C. D., "Steel Fiber Reinforced Mortar and Concrete: A Review of Mechanical Properties", Fiber Reinforced Concrete, SP-44, American Concrete Institute, Detroit, 1974.

9. Meinheit, D. F., and Jirsa, J. O., "The Shear Strength of Reinforced Concrete Beam-Column Joints", Report No. 77/1, Department of Civil Engineering, Structures Res. Lab., University of Texas at Austin, January 1977.

10. Millburn, J. R., and Park, R., "Behavior of Reinforced Concrete Beam-Column Joints Designed to NZS 3101", Report No. 82-7, Department of Civil Engineering, University of Canterbury, Cristchurch, New Zealand, February 1982.

11. Otter, D. E., and Naaman, A. E., "Fiber Reinforced Concrete Under Cyclic and Dynamic Compressive Loadings", Report No. UMCE 88-9, Department of Civil Engineering, The University of Michigan, Ann Arbor, October 1987.

12. Popov, E. P., "Seismic Behavior of Structural Subassemblages", Journal of the Structural Division, ASCE, Vol. 106, ST7, July 1980.

13. "Recommended Lateral Force Requirements and Commentary", Seismology Committee, SEAOC, San Fransisco, 1980.

14. Shah, S. P., and Naaman, A. E., "Mechanical Properties of Glass Steel Fiber Reinforced Mortar", ACI Journal, Proceedings, Vol. 73, No. 1, January 1976.

15. Swamy, R. N., Mangat, P. S., and Rao, C. V. S. K., "The Mechanics of Fiber Reinforcement of Cement Matrices", Fiber Reinforced Concrete, SP-44, American Concrete Institute, Detroit, 1974.

16. Townsend, W. H., and Hanson, R. D., "Reinforced Concrete Connection Hysteresis Loops", ACI Publication SP-53, Symposium on Reinforced Concrete Structures in Seismic Zones, 1974 ACI Annual Convention.

17. Uniform Building Code, 1982 Edition, International Conference of Building Code Officials, Wittier, California, 1982.

18. Uzumeri, S. M., "Strength and Ductility of Cast-in-Place Beam-Column Joints", ACI Publication SP-53, Symposium on Reinforced Concrete Structures in Seismic Zones, 1974 ACI Annual Convention.